12-2016

Measuring the Effects of High-Altitude Flight and Upper Atmospheric Radiation on Muscle Cells

Annelise Dykes
Utah State University

Measuring the Effects of High-Altitude Flight and Upper Atmospheric Radiation on Muscle Cells

by

Annelise Dykes

Thesis submitted in partial fulfillment of the requirements for the degree

of

Departmental Honors in Biological Engineering

in

Biological Engineering
in the Department of Biological Engineering

Approved:

Thesis/Project Advisor
Dr. Elizabeth Vargis

Departmental Honors Advisor
Dr. V. Dean Adams

Director of Honors Program
Dr. Kristine Miller

UTAH STATE UNIVERSITY
Logan, UT

Fall 2016

Measuring the Effects of High-Altitude Flight and Upper Atmospheric Radiation on Muscle Cells

Lori Caldwell, Annelise Dykes, Katherine Glaittli
Dr. Elizabeth Vargis, Charles Harding

14 December 2016
Department of Biological Engineering
Utah State University

Table of Contents

List of Figures

List of Tables

Abstract

There are several physiological barriers to long-term space travel, including the effects of launch, landing, and microgravity on muscle cells. A payload capsule was designed to maintain cell growth during a high altitude balloon flight to model some of these physiological processes. Murine muscle cells (strain C2C12) were cultured and launched in a capsule on a balloon satellite in November 2016. Cells were monitored for changes due to temperature, flight motion, radiation, and gravity differences by quantifying cell characteristics before and after the flight using physical measurements and cell viability. Instruments were selected to monitor flight data, and a payload capsule was designed for cell survival by maintaining a constant temperature of 37°C and redistributing impact forces.

Introduction

As longer space missions become more desirable to public and private institutions, the physiological impact on astronauts must be considered. One of the primary concerns for those spending time in low-gravity environments is the eventual loss of muscle tissue due to atrophy, because a decreased force pulling on muscle fibers leads to marked atrophy in as little as nine days. This debilitating loss of muscle makes it difficult for homeward-bound astronauts, who are returning to full gravity, to regain their physical strength.

Studies of rats immobilized by hindlimb suspension have indicated that protein synthesis decreases drastically during the first four hours of immobilization. This decrease in protein synthesis causes oxidative stress, triggering an increase in proteolysis within the limb (Powers, 2005). Oxidative stress is exacerbated by radiation, making reactive oxygen species a particular concern for astronauts.

The aim of this project was to study the effects of spaceflight and radiation on muscle cells. A payload was designed to maintain cell life and was sent to the ozone layer of the stratosphere, where it received approximately 12 μSv/hr of gamma radiation. This facilitated the comparison of high-altitude flight data to data collected from a rotary cell culture apparatus simulating microgravity.

Problem

Space travelers experience significantly less gravity in space than on earth which leads to muscular atrophy in both skeletal and smooth muscle. This then becomes a problem upon return to Earth when astronauts are no longer as strong as their pre-expedition levels. In particular, the heart loses muscle mass in microgravity and may have trouble pumping a sufficient amount of blood to the body upon return to full gravity. Current solutions for this problem include intense exercise regimens both before and during space flight to build and maintain muscle mass as much as possible. Cell-based studies have been conducted on the

International Space Station to explore the effects of microgravity and radiation on atrophy. These trials are both costly and difficult to get approval for. A low atmosphere capsule would enable researchers to study the impacts of flight on cell growth. This study examines the effect that gamma radiation and high-altitude flight have on muscle cells.

Significance and Innovation

Deep space exploration has recently become a highly researched field as space travel has become a more realistic option. There has been significant data collected on the biological effects on astronauts after spending time in microgravity, one of them being muscle atrophy. As the possibility of long-term spaceflight and colonization of other planets with smaller gravitational fields is considered, preventative measures for muscle atrophy need to be explored so astronauts can maintain their physical health throughout the duration of their expedition.

The goal of this project is to design a capsule to launch muscle cells into the ozone layer. This will allow for further research on how fibers are affected and what damage occurs when exposed to solar radiation 20+ kilometers up into the atmosphere. Ground level simulations have been done, but it measuring all of the effects simultaneously has proven difficult without an actual launch. This data may help in discovering new methods of atrophy prevention while in microgravity conditions.

In order to perform these tests, a lightweight pod that can house the muscle cells in an optimal environment was designed. The design used utilizes heating pads and aluminized mylar to maintain a temperature of 37°C, a nylon suspension system to hold the cell flasks, and a frangible outer container to absorb the forces experienced on impact. A weather balloon was used to facilitate the flight, and a tracking system was used to collect flight data and recover the payload.

Objectives

The overall goal of this project was to design a pod that could be launched into the ozone layer to compare to simulated microgravity and radiation in a laboratory. The following criteria were used:

- Pod was lightweight enough to be launched with a 1200 gram weather balloon
- Cells stay alive throughout the duration of the flight

Evaluation Criteria

To achieve the objectives listed above, the payload will be evaluated based on the following factors:

- Ability to maintain a constant temperature of 37°C ∓ 10°C
- Weight less than 6 pounds (2.73 kg)
- Ability to insulate cells from flight and landing forces measured using cell viability, must be greater than 50% after flight
- Reach an altitude of 20km (the ozone layer)
- Ability to track flight path
- Ability to recover payload for analysis

Background

Properties of Muscle Cells

Skeletal muscle cells, or fibers, are characterized by their striations and multinucleation. Contraction of the muscle fibers occurs through action potentials starting a chain reaction that results in the myosin heads attaching to actin binding sites which pull the Z bands together, thus contracting or shortening every sarcomere in the muscle fiber as seen in Figure 1.

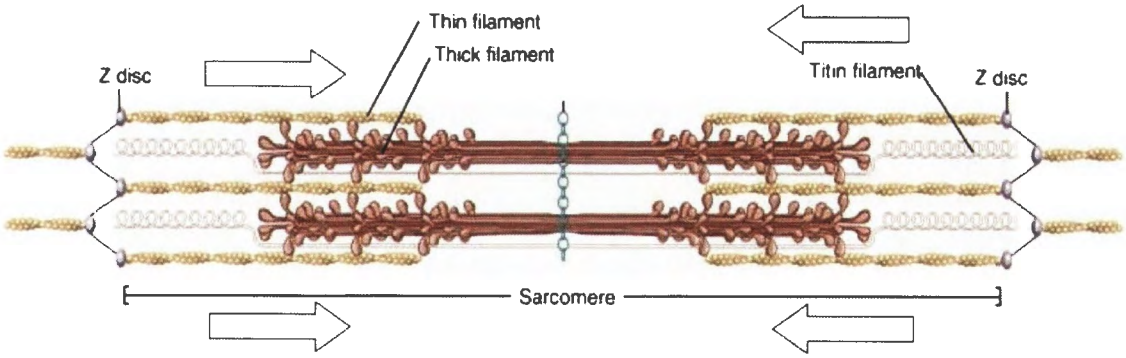

Figure 1. Sarcomere representing muscle contraction through the attachment of myosin heads to actin binding sites, pulling the Z bands towards the M line (represented in blue, not labeled.) Courtesy of https://thetmonitor.wordpress.com/2012/09/10/rigor-mortis-and-protein-sex/

Skeletal muscle cells make up 40% of muscle tissue in the human body. Each individual skeletal muscle fiber is separate from those surrounding it and runs parallel to along the skeletal muscle tissue. Cardiac muscle cells are characterized by striation, intercalated discs, gap junctions, and are found exclusively in the myocardium of the heart wall. Contraction is similar to that of the above sarcomere, with the exception being cardiac muscle fibers are

interconnected for systemic contraction. This allows the atrium to contract as a whole followed by the ventricle for a decreased probability of electrical failure.

Muscle Atrophy

Space travel may cause muscle atrophy as seen in Figure 2 by altering circulating levels of factors such as growth hormone, glucocorticoids, and anabolic steroids and/or by a direct effect on the muscle fibers. Powers et.al cultured and monitored muscle cells aboard the International Space Station and found significant atrophy. A decrease in protein synthesis rates accompanied the atrophy, although no increase in protein degradation occurred.

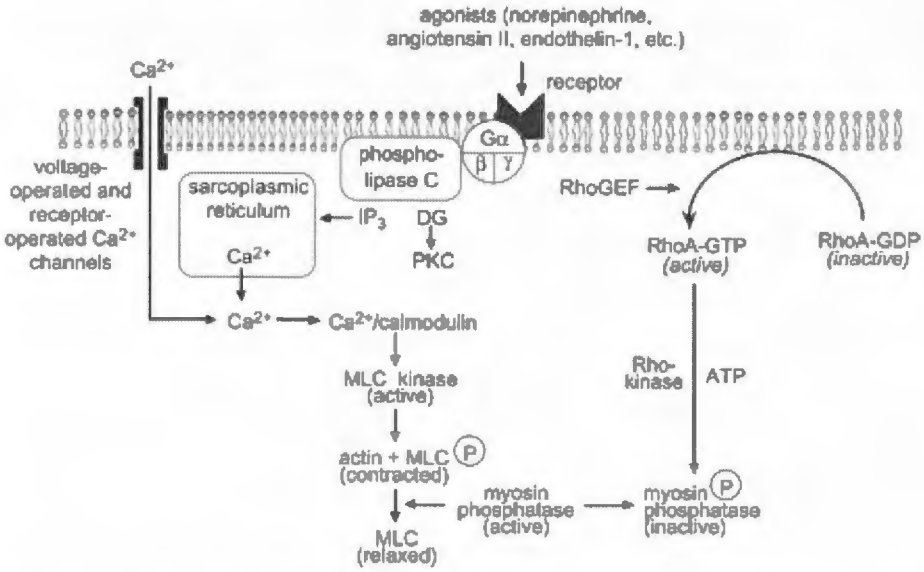

Figure 2. Regulation of smooth muscle contraction. Various agonists (neurotransmitters, hormones, etc.) bind to specific receptors to activate contraction in smooth muscle (Webb, 2003).

Skeletal muscle has evolved as a tissue whose primary function is to move objects against the force of gravity, and there is a close relationship between the size and metabolism of this tissue and gravitational force. When a heavy object is moved repeatedly, the muscle cells enlarge by hypertrophy, whereas a reduction in muscle tension or use, as occurs in bedridden patients and astronauts in space, leads to rapid skeletal muscle wasting as seen in Figure 3. Muscles use two different mechanical forces to overcome gravity namely, active and passive. Active muscle tension occurs during muscle contractions and results in a shortening of the sarcomere. Passive muscle tension occurs during stretching and results in a lengthening of the sarcomere. Both tension types are essential for normal muscle growth as the loss of either force leads to muscle atrophy.

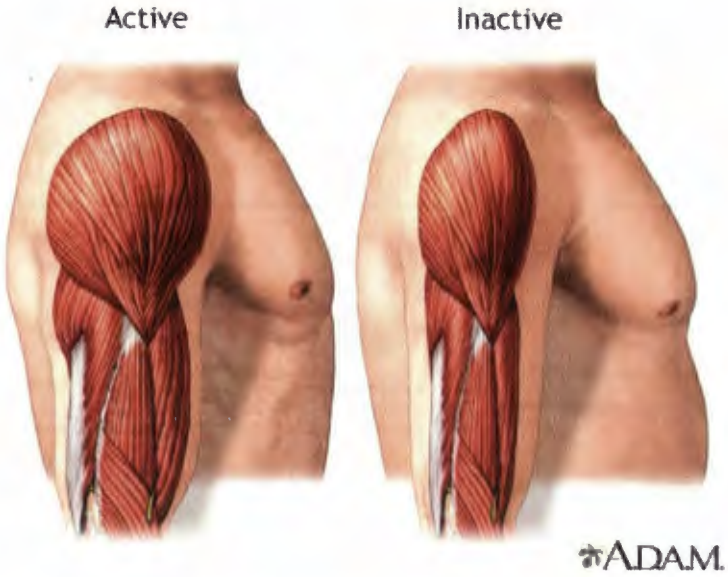

Figure 3. Atrophy of upper arm muscles due to disuse or extended time in a microgravity environment.

Radiative Effects

The approximate radiation dosage at ground level is 0.3 μS/hr causing minor damage to cells that is quickly repaired. For astronauts on the International Space Station, the radiation can read as high as 18.2 μS/hr. At about 30 km above ground in the stratosphere, the radiation exposure is approximately 12 μS/hr. Measuring the DNA dosage and understanding radiation effects on cells growth and reproduction can contribute to preventing radiation damage in future explorations.

Ionizing radiation is composed of alpha particles, beta particles, and gamma rays. Damage to astronauts comes mainly from gamma rays since the metal exterior of the ISS and their flight suits block both alpha and beta particle penetration. DNA damage occurs when gamma rays break hydrogen bonds between single strands and individual amino acids. Cells are unable to repair the damage quickly enough to prevent long term problems from occurring while outside Earth's atmosphere. Types of damage to the DNA include deletion of one to millions of nucleic acids in the DNA sequence, altering nucleic acids leading to incorrect translation, and breaking the sugar-phosphate backbone as a single strand break (SSB) or a double strand break (DSB). An SSB can be repaired relatively quickly depending on cell type, age, and the extracellular environment. A DSB is more critical and causes the majority of the problems that occur such as genomic instability, cell death, and cancer as seen in Figure 4.

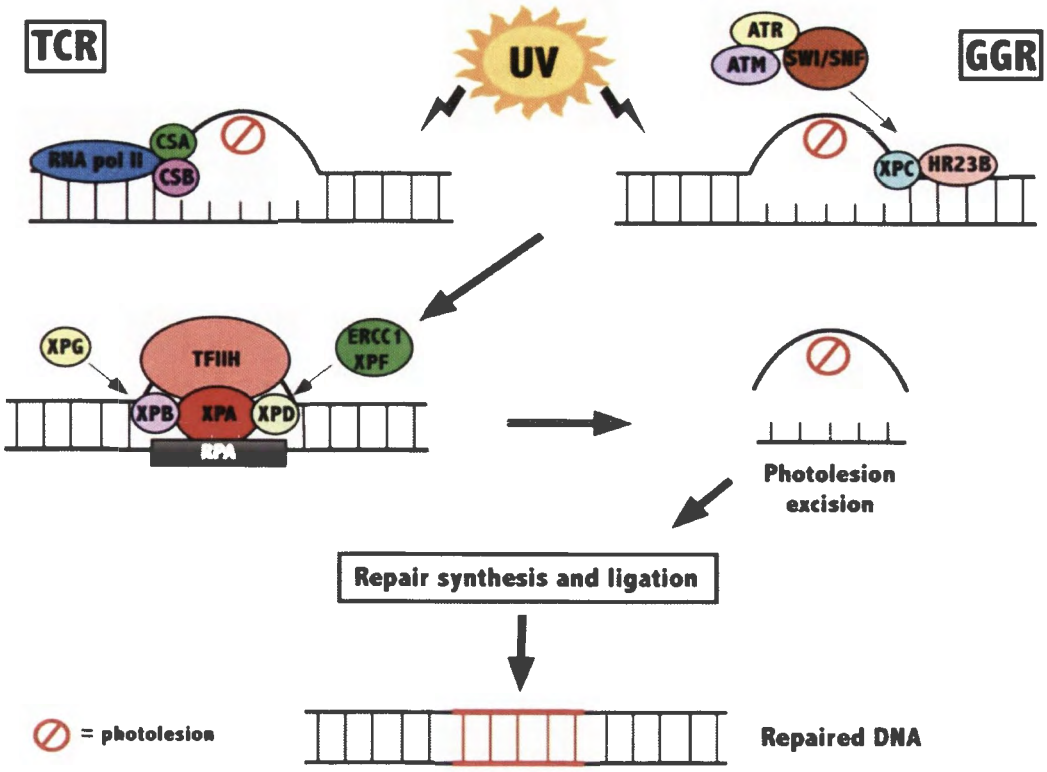

Figure 4. UV radiation results in damage to cell DNA preventing transcription and causing genomic instability. DNA repair is a result of multiple proteins and hormones working together; this mechanism is hindered in space due to hormonal imbalances (Farrell, 2011).

There is a significant amount of new research on the effects of ionizing radiation on oxidation reactions and cellular responses. Spitz et al. discuss the exposure of eukaryotic cells to ionizing radiation resulting in the formation of free radicals such as hydroxyl radicals (·OH), superoxides (·O.), and organic radicals (·R) for a relatively short period of time (milliseconds). The short period of time was enough to cause lasting oxidative damage in the cell causing an increase in the expression of cellular antioxidant defenses. They also found that ionizing radiation can disrupt the assembly and function of electron transport chains in the mitochondria through heritable mutations to the DNA that can affect daughter cells and animal offspring.

Simone et al. suggest two causes for severe cellular damage through IR: 1) direct damage through disruption of DNA integrity and 2) indirect damage as a result of free radical formation. They explored microRNA (miRNA) which is involved in regulating the genes that respond to potential lethal stressors, such as IR. They exposed cultures to 0.25, 0.5, 0.75, 1, 3, 5 and 10 cGy/min of IR and found that damage increased along with the IR dosage (Simone, 2009).

Yatagai et al. exclusively measured radiative effects on the International Space Station by keeping lymphoblastoid TK6 cells frozen at -80°C for a total flight time of 134 days. Keeping the cells frozen eliminated all launch stress effects and microgravity effects (Yatagai, 2010). They found that the cells were exposed to 0.54 mSv per day, reaching a total of 72 mSv for the duration of the flight. To contrast, ground level radiation is 2.4 mSv per year. They also discussed the radiation field at low earth orbit that contains radioactive particles such as protons, α-particles and heavy ions (up to iron). In addition, the secondary radiation emitted from the formerly mentioned particles are categorized as primary cosmic rays.

Microgravity Effects

Many physiological changes have been shown in muscle cells cultured in microgravity environments. These include weakening of contractile performance, loss of detectable mitochondrial functionality, an erosion of myofibrils from sarcomeres, a decrease in myosin ATPase activity, and shifts in predominant metabolic pathways for the provision of energy to support contraction (Kulesh, 1994). These effects can also occur rather quickly. Figure 5 displays a difference in gene expression after only 12 hours of simulated microgravity conditions (Damm, 2013).

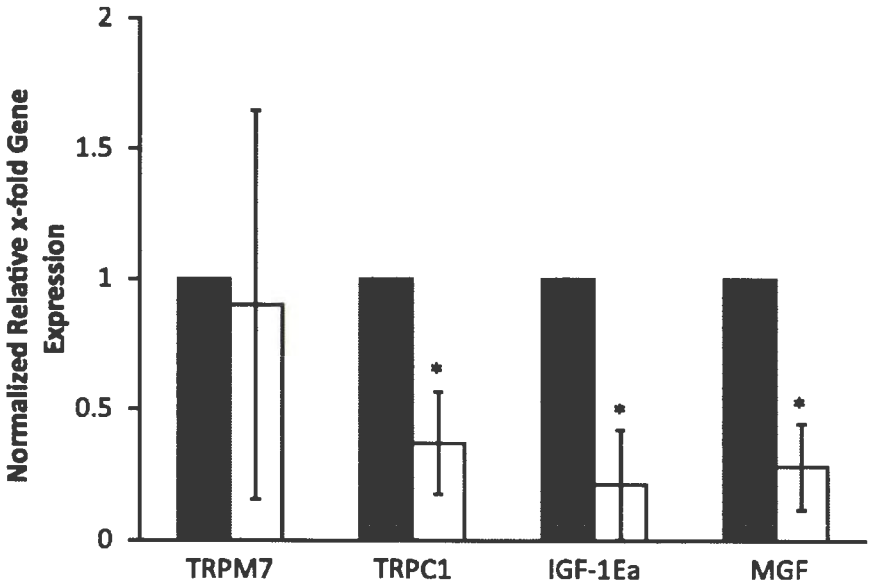

Figure 5. Calcium-regulated transcriptional events are decreased after only 12 hours in microgravity (Damm, 2013). The black bars show the expression of genes before being subjected to microgravity, and the white bars show the expression of genes after being subjected to microgravity. The specific genes are listed below the graph.

Research conducted by Charles Harding at Utah State University includes culturing muscle cells in a microgravity simulation using a rotary cell culture device as seen in Figure 6.

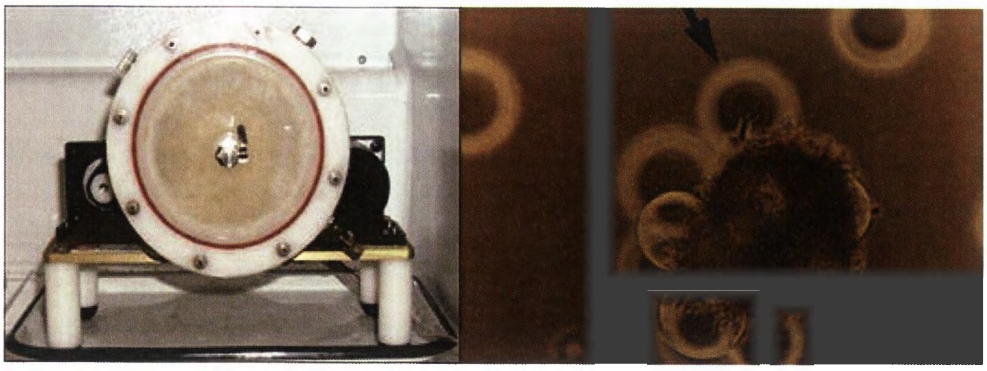

Figure 6. Left - microgravity simulating bioreactor spins on a central axis to keep cells in freefall. Right - tumor cells growing on microcarrier beads within the bioreactor after 2 days ("The Cure", 2013).

Design Process

Rationale

The goal for the final product was a system that would allow for the study of flight forces and landing impacts on cultured cells. This included designing a system that would take the cells on a short flight to the stratosphere, making sure the cells were insulated from the impact of landing, selecting instruments to record data about the flight, designing a tracking system so the payload could be recovered, and keeping the cells alive during the flight.

To evaluate the product, cells needed to be grown in an amount sufficient for analysis. In order to do this, a trial of cell growth on different substrates was conducted. The final substrate decision was based on differentiation and confluence of muscle cells on each substrate.

The final product also needed to record information about altitude, flight path, temperature, and radiation. This would allow for a more detailed study of which forces would impact the cells. Each sensor was selected based on compatibility with a microcontroller, ability to record the necessary range of data, and ability to withstand flight forces.

A microcontroller was selected to connect to the relevant sensors and record data. Selection was based on the instruments that could be connected and overall cost.

The capsule needed to insulate the cells from the cold temperatures encountered in the stratosphere, maintain a constant temperature of 37°C, and insulate the cells from the forces of launch and landing to keep the cells alive during the launch, flight, and landing. The final design decision was made based on the ability to meet the listed criteria while staying under a weight of 6 lbs.

Decisions

The following sections detail which decisions were made for each part of the final product and why they were made. The final decision for each category is highlighted in yellow. Mann-Whitney U tests were used to prove that the final decisions were appropriate. The Mann-Whitney test was selected instead of a standard t-test because Mann-Whitney tests compare the rankings of one set of data to another set of data, instead of using the mean. It also does not require the assumption that the data is normally distributed. In order to ensure the accuracy of the results, rankings for each item were decided by a different individual than the one that did the statistical analysis. It should be noted that since the sample size of these rankings was small, the p-values do not reach a significance level of $\alpha=0.05$. Thus, the decision was considered valid if the p-value showed that the difference in rankings approached significance.

Cell Culture Substrate

An analysis of polystyrene, polysulfone, polyethersulfone, and decellularized collagen was done to determine which would best facilitate cell growth. In order to maximize the number of cells, different arrangements for growth, such as layers of flat plates or hollow-fiber membranes were also considered. In the end, it was determined that cells grew best on plasma-treated polystyrene, which cannot be formed into hollow-fiber membranes. Two T-12.5 flasks were attached together to give more surface area for cell growth. Images from these analyses can be found in the results section.

Sensors

Sensors to monitor and control the payload environment were chosen and connected to the microcontroller. Details of the sensor decisions are included in Table 1 with a numerical ranking based on weight, accuracy, required amperage, and cost.

Table 1. Decision matrix for payload sensors.

Type	Amperage required	Weight	Benefits	Drawbacks	Numerical Ranking
COM 11288 ROHS heating pad	~750 mA **3/10**	25 g **4/10**	Lightweight, size of flask, inexpensive, consistent heat **7/10**	Relatively high amperage required	**14/30**
Flexible silicone heating pad	~370 mA **6/10**	14 g **6/10**	Lightweight, low amperage required **6/10**	Expensive, variable heat output, requires adaptor to use with microcontroller	**18/30**

Type	Amperage required	Weight	Benefits	Drawbacks	Numerical Ranking
SEN 11050 ROHS temperature sensor	~25 mA **9/10**	12 g **7/10**	Waterproof, long connector cable, only needs one input port **7/10**	Moderately expensive, requires amplifier	**23/30**
SEN 10988 ROHS temperature sensor	~40 mA **8/10**	3 g **10/10**	Lightweight, highly accurate **8/10**	Requires 3 input ports	**26/30**
SEN 10167 ROHS humidity and temperature sensor	1.0 - 1.5 A **1/10**	14 g **6/10**	Dual measurement **7/10**	Relatively heavy, requires 4 input ports, requires high amperage	**14/30**
SEN 12872 pH sensor	~900 mA **1/10**	125 g **1/10**	High accuracy **5/10**	Heavy, expensive, requires adaptor for microcontroller	**7/30**

It was decided to use two COM 11288 ROHS heating pads to sandwich the cell flasks because they provide a more consistent heat output than the flexible silicone heating pads. The SEN 11050 ROHS temperature sensor was chosen to monitor the external environment because it is waterproof and has a long cable to span the payload and protective casing. The SEN 10988 ROHS temperature sensor was chosen to monitor the interior payload temperature because it is capable of measuring every second and has a narrow margin of error in measurements. This decision was justified by a Mann-Whitney U test p-value of 0.0171.

Microcontroller

The use of a microcontroller was necessary to control the temperature sensors, heating pads, and data logger. A temperature sensor was included in the cell chamber to send feedback to the microcontroller which in turn increased heating in the chambers by powering electric heating pads. Also included in the cell chamber were four handwarmers to reduce the power load on the heating pads. An external temperature sensor monitored the ambient temperature of the payload. Research on different types of microcontrollers is shown in Table 10 with numerical rankings based on availability, cost, weight, and compatibility with chosen sensors.

Table 2. Research on types of microcontrollers ("Microcontroller Basics", 2013)

Type	Pros	Cons	Numerical Ranking
8051 microcontroller (Arduino and Raspberry Pi)	• 3 timers • 4kb ROM • 128 bytes RAM • 4 parallel 8 bit ports	• Must add external storage (up to 64 KB) • No USB available	**9/10**
PIC (peripheral interface controller) microcontroller	• Low cost • 6 - 28 pins available • Ideal for battery enablization • USB ports available	• Have to purchase each "upgrade" (i.e. USB port)	**3/10**
AVR (advanced virtual RISC) microcontroller	• Programs and data are stored in separate spaces • Incorporated SRAM and Flash	• No external memory available • No USB available	**1/10**
ARM microcontroller	• Simple programming • Power-saving attributes	• No support for misaligned memory access	**5/10**

It was determined that the best type of microcontroller for this project was an 8051 because it would interface with a wide range of sensors. Extensive programming tutorials are also available for both Arduino and Raspberry Pi. The Arduino UNO, specifically, was selected because it is the smallest and most basic of the available options, but still had enough pins to

connect the necessary elements. This decision was justified by a Mann-Whitney U Test p-value of 0.1797.

Radiation Monitoring

Accurate radiation dosage levels received by the experimental flask were necessary to do quantitative analysis on cell changes between the control and experimental trials. Radiation monitoring techniques are detailed in Table 3 with the chosen method highlighted in yellow. Numerical rankings were assigned based on accuracy, weight, cost, and data analysis tools.

Table 3. Decision matrix for radiation monitoring method.

Method	**Accuracy**	**Weight**	**Cost**	**Analysis**	**Numerical Ranking**
Film Badge	Medium **5/10**	Low **10/10**	High **1/10**	Dosage must be read by unavailable instrument **1/10**	**17/40**
Personal Dosimeter	High **10/10**	Medium **5/10**	High **1/10**	CSV output **5/10**	**21/40**
Measurement Probe	Medium **5/10**	Medium **5/10**	Medium **5/10**	Stores data and exports to CSV file **5/10**	**20/40**
Radex RD 1212 Geiger counter	High **10/10**	Low **10/10**	Medium **5/10**	Sends reading to web **1/10**	**26/40**
GQ GMC 300 Geiger counter	High **10/10**	Low **10/10**	Low **10/10**	CSV output **5/10**	**35/40**
Smart Geiger radiation detector	Medium **5/10**	Low **10/10**	Low **10/10**	Connects to smartphone (unavailable in atmosphere) **1/10**	**26/40**

It was decided to use the GQ GMC 300 Geiger counter to measure radiation because it is lightweight (6.8 oz), stores data internally and exports to a CSV file, and measures exposure in CPM (counts per minute). The benefit to measuring exposure in CPM instead of uS/hr is that a CPM measurement can be converted into a dosage if the particle type is known and a particle density map can be created based on the timestamp on each reading. This decision was justified by a Mann-Whitney U Test p-value of 0.1123.

Payload Insulation

To minimize heat loss and energy required for the heating pads, the payload was insulated with a layer of aluminized Mylar, cardboard, and a secondary layer of aluminized mylar on the

interior surface of the Styrofoam container. The decision to use this material is outlined in Table 4 with the chosen material highlighted in yellow. Numerical rankings were assigned based on weight, insulation properties, cost, and radiation shielding properties.

Table 4. Decision matrix for internal payload insulation material.

Material	**Weight**	**Insulation**	**Cost**	**Shielding**	**Numerical Ranking**
Water	High **1/10**	Medium **5/10**	Low **10/10**	Shields gamma radiation **10/10**	**26/40**
Spray insulation	Medium **5/10**	Medium **5/10**	Low **10/10**	None **1/10**	**21/40**
Aluminized mylar	Low **10/10**	High **10/10**	Low **10/10**	Shields alpha and beta particles **5/10**	**35/40**
Fiberglass	Medium **5/10**	Medium **5/10**	Medium **5/10**	None **1/10**	**16/10**
Air pillows	Low **10/10**	Low **1/10**	Low **10/10**	None **1/10**	**22/40**
Aluminum coated bubble roll	High **1/10**	High **10/10**	High **1/10**	Shield alpha and beta particles **5/10**	**17/20**
Cardboard	Medium **5/10**	Medium **5/10**	Low **10/10**	None **1/10**	**21/10**

It was decided to use aluminized mylar as interior insulation for the payload because it is lightweight, inexpensive, an excellent insulator, and provides shielding from alpha and beta particles - similar to material used in the fabrication of the International Space Station and astronaut's space suits. Spray adhesive was used to adhere the mylar and cardboard to the styrofoam container. This decision was justified by a Mann-Whitney U Test p-value of 0.1960.

Protective Casing

Since an objective of the payload was to protect the cells, and the cells in the payload container are delicate and can be damaged from seemingly minor impacts, a protective shell was designed. To be included, the shell needed to be less than 2 pounds, absorb enough force from the landing impact to cushion the cells, and remain with the payload in the event of a catastrophic failure. The major iterations of the protective shell design are included in Table 5 with the chosen design highlighted in yellow. Numerical rankings were assigned based on weight, frangibility, cost, and consistent reproducibility.

Table 5. Decision matrix for external protective casing of payload design.

Material	**Weight**	**Frangibility**	**Cost**	**Reproducibility**	**Numerical Ranking**
Carbon fiber rods (rectangular pyramid)	Medium **5/10**	Medium **5/10**	Medium **5/10**	Difficult **5/10**	**20/40**
Fiberglass rods (rectangular pyramid)	Medium **5/10**	Medium **5/10**	Low **10/10**	Difficult **5/10**	**25/40**
Styrofoam box	Low **10/10**	Low **1/10**	Low **10/10**	Easy **10/10**	**31/40**
Styrofoam cube matrix	Low **10/10**	High **10/10**	Low **10/10**	Highly difficult **1/10**	**31/40**
Nylon reinforced plastic bag with styrofoam peanuts (closely packed)	Low **10/10**	High **10/10**	Low **10/10**	Easy **10/10**	**40/40**

It was decided to use a nylon reinforced plastic bag packed closely with styrofoam peanuts to cushion the payload from impact forces. To ensure that the payload maintained a centered position within the bag, the payload was suspended in a net. The exterior protective shell was attached directly to the payload and the net so as to remain with the payload in the event of failure - the payload detaching from the balloon and parachute. Compostable packing peanuts were used to fill the reinforced bag to minimize environmental impacts should the bag tear on impact. This decision was justified by a Mann-Whitney U Test p-value of 0.0890.

Flight System

The main objective of this project was to design a payload system to protect living cells during flight. In order to test this, an analogy of spaceflight was chosen. During a spaceflight, cells would encounter jarring motions, rapid ascent/descent, high G-forces during takeoff, and microgravity during flight. Since no system other than a rocket launch and flight accurately mimics all of these parameters, it was decided to focus specifically on recreating jarring motions and a rapid ascent and descent. The decision process for the flight system is outlined in Table 6 with the chosen material highlighted in yellow. Numerical rankings were assigned based on lift, flight time, similarity to space flight, and cost.

Table 6. Decision matrix for flight system to carry payload.

System	Lift	Flight Time	Similarity to space flight	Cost	Numerical Ranking
Weather balloon	~ 6 pounds **5/10**	1 - 3 hours **5/10**	Medium **5/10**	Low **10/10**	**25/40**
Cubesat	< 3 pounds **1/10**	Indefinite **5/10**	High **10/10**	High **1/10**	**18/40**
Hot air balloon	> 500 pounds **10/10**	0.5 - 3 hours **3/10**	Low **1/10**	Medium **5/10**	**18/40**
Shaker plate	NA	NA	Low **1/10**	Low **10/10**	**11/40**
Drone flight	~ 6 pounds **5/10**	< 1 hour **3/10**	Medium **5/10**	High **1/10**	**14/40**

A weather balloon was chosen as the flight mechanism for the designed payload because of its simple tracking and retrievability and it's relatively long flight time compared to other options. When filled with 300 liters of helium gas the balloon ascends at a rate of approximately 7 m/s, much lower than a rocket but high enough to cause jarring motions within the payload. After bursting, the payload descends at a rate of approximately 17 m/s. This decision was justified by a Mann-Whitney U Test p-value of 0.2220.

Parachute

A 4 ft in diameter rip-stop nylon parachute was attached directly beneath the balloon to reduce the impact velocity of the payload. The bottom corners of the parachute were attached to a small hula-hoop, approximately 3 ft away, to aid the parachute in opening after the balloon burst. The parachute was attached to the balloon by folding the neck of the balloon in half through a loop attached to the parachute, then zip-tying the neck of the balloon closed. The zip ties were wrapped in electrical tape to prevent the edges of the ties from snagging on the balloon or parachute. The general attachment setup is shown in Figure 7.

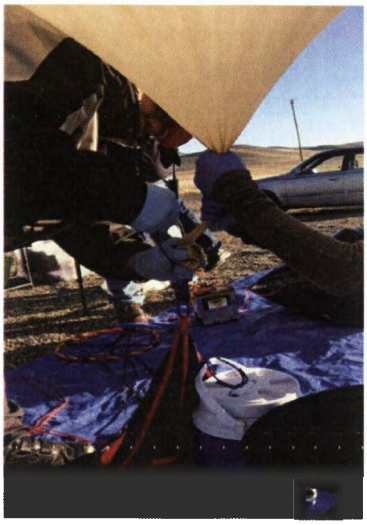

Figure 7. The parachute was attached to the balloon by folding the neck of the balloon through a nylon rope loop then zip-tying the balloon closed. The ties were covered with electrical tape to prevent the edges from snagging on the balloon or parachute.

This particular parachute was chosen because of it's availability and reliability in previous flights performed by Dr. Reeve's high-altitude balloon hobbyist group.

Tracking System

Dr. Kevin Reeve (USU Distance Ed Department) provided a tracking system that had been used multiple times previously with no failure. The system consisted of a specialized GPS monitor that was rated for altitudes up to 150,000 ft and reported a location every 80 seconds as well as a radio transmitter that relayed to aprs.fi under the callsign "USUBE" every 10 seconds. The tracking system was enclosed in a box as shown in Figure 8.

Figure 8. The tracking system provided by Dr. Reeve contained both a GPS and radio transmitter that updated on aprs.fi under the callsign "USUBE."

The GPS was used primarily as a failsafe for the radio transmitter since it becomes unreliable on the ground. The radio signal was triangulated using HAM radios to locate the payload after it had landed.

Design Testing and Results

In order to effectively design the capsule, it was necessary to test multiple aspects of the project. The first step was growing cells and determining which substrate would best promote cell growth and differentiation. Since radiation in the upper atmosphere is significantly higher than on Earth's surface, the cells were exposed to a simulated high altitude radiation dosage using cesium disks. One problem encountered in sending cells to the upper atmosphere was that anything in a low-pressure atmosphere requires a closed environment. Since there would be no oxygen or carbon dioxide exchange in the payload, cells were grown and sealed in a flask filled with media then left for 24 hours in the incubator to test viability and pH before and after the trial. After it was determined the cells could survive without air exchange for at least 24

hours, a microcontroller was built to maintain homeostasis within the payload. The efficacy of the temperature control system was tested by placing the sealed payload in a -20°C freezer and storing temperature readings over six hours for further analysis. To determine whether the payload could insulate cells from impact effectively, an impact experiment was designed. Flasks of cells were filled with media and sealed in the payload, then dropped from a height calculated to have the same impact velocity as the prediction based the UK HabHub society's flight prediction algorithm (HabHub 2015). Details about these tests are given below.

Cell Culture Trials

To correctly analyze the impacts of launch, flight, and landing on the cells it was necessary to have healthy, attached cells. Cell growth trials began in March 2016 and concluded in August 2016. The original cell growth goal was to grow as many cells as possible in a small space so that GeneChip analysis could be done to measure DNA damage in the cells. However, as the project progressed, radiation testing in the laboratory showed that the amount of DNA damage could not be detected with GeneChip analysis. This, in addition with the high cost of GeneChip analysis, caused the goal of the project to shift to growing healthy cells that could be observed easily with a microscope and used in a Trypan Blue© assay. Even though the original plan was altered, the results of these cell growth trials on different substrates were still used to determine which substrate would best support cell growth.

Initial Cell Culture Trials

In order to practice cell culturing technique, a few trials of standard cell growth on tissue-culture polystyrene were done. In these trials, C2C12 myoblast cells were seeded at 100,000 cells/ml in Falcon® T25 cm^2 tissue culture treated polystyrene flasks and maintained using DMEM-F12 10% FBS for 3 days then DMEM-F12 5% FBS for the remainder of the experiment to encourage cell differentiation.

Cells grown in Trial 1 exhibited good attachment and viability, but did not fully differentiate after 12 days of growth as seen in Figure 9.

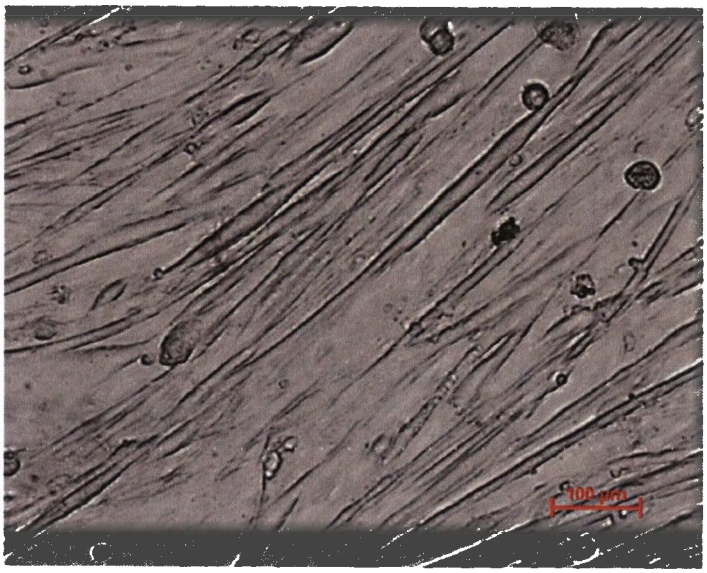

Figure 9. C2C12 myoblast cells grown in Falcon® T25 cm^2 flasks seeded at 100,000 cells/ml exhibited good attachment and viability after 12 days of growth. Cells did not fully differentiate into myotubes. Scale = 100 µm.

After discussion with Dr. Vargis, and Charles Harding, it was suspected that the reason for this result was the cells had been passaged too many times. Because of this, a second trial was done to perfect the technique.

The same procedure was followed in the second trial for cell growth. However, the cells did not grow well and also did not differentiate well. The results from this trial are shown in Figure 10.

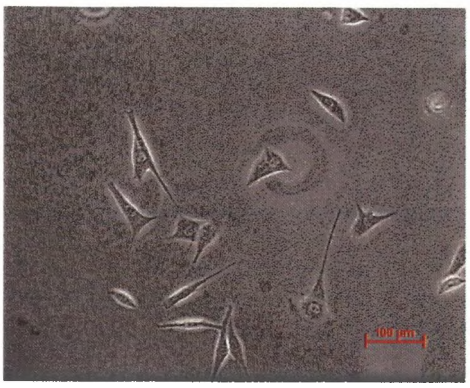

3/23/16 Day 2

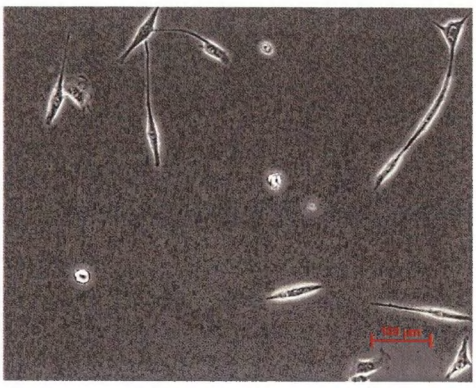

3/25/16 Day 4

3/28/16 Day 7

Figure 10. Cells in Trial 2 showed no significant growth 7 days after seeding.

On Day 8 of this trial, it was discovered that the reason for the lack of growth was that the flasks were non-vented, and needed to be opened slightly in order for oxygen to reach the cells. A third trial was then done with unvented flasks.

Cells grown in Trial 3 followed the same protocol as Trials 1 and 2, but used cells that had been passaged fewer times and vented flasks. The results of this trial are shown in Figure 11.

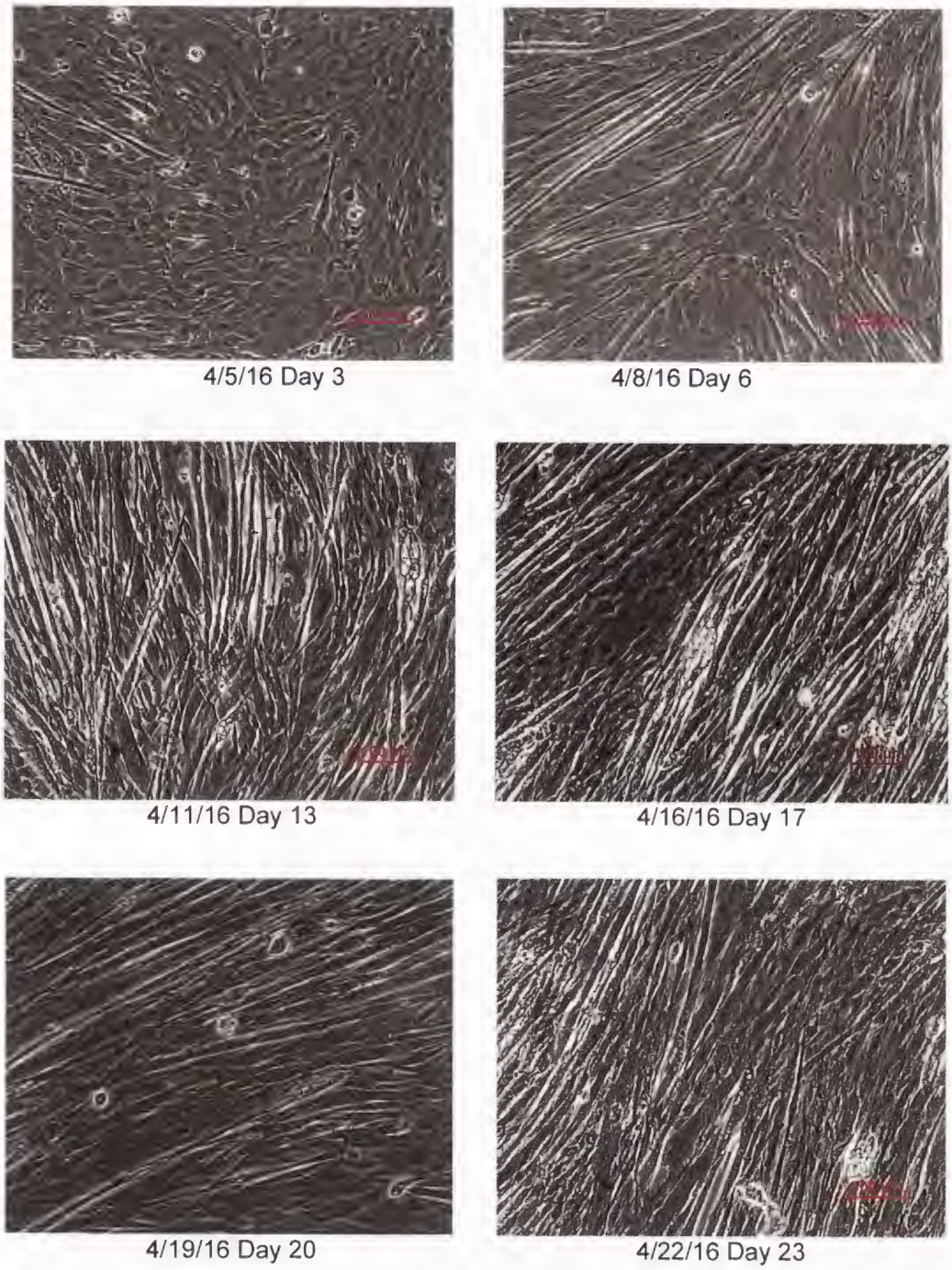

Figure 11. Cells were maintained in DMEM 2% FBS; the media was changed every third day. Cells showed distinct striation patterns, indicating proper cell differentiation, beginning day 6.

The cells in Trial 3 showed good attachment, viability, and differentiation over a 23 day growth period as seen in Figure 11. This result showed that the procedure for cell growth could be

finalized and tests could be done on different substrates. The cells were cryopreserved after 23 days of growth.

Cryopreservation of Cells

Since the cells had grown and differentiated well in Trial 3 of the initial cell culture trials, the cells were cryopreserved at 23 days. This prevented loss by contamination, minimized genetic change, and allowed the cells to avoid aging and transformation ("Cryopreservation," 2014). It also built an available stock for cell growth on different substrates, additional trials, and the final launch. The cryopreservation was done according to the following procedure:

Materials

- Cells
- Trypsin 0.25%
- DMEM 10% FBS 10% DMSO
- Liquid Nitrogen
- 50mL centrifuge tube
- Cryovial

Methods

1. Scale up the cells to make the desired number of vials at 1E6 cells per vial.
2. Trypsinize all the stock flasks as normal and combine the cells into one 50mL centrifuge tube.
3. Re-suspend the cells in DMEM 10% FBS 10% DMSO such that the cell density is 1E6 cells/mL
4. Add 1 mL per cryovial, label, and place in the cryo freezing container. Make sure the container has the proper volume of ethanol.
5. Store the freezing container at -80C overnight.
6. Move the cells to a cardboard box and store in the LN2 tank.

Cell Culture Trials on Varying Substrates

Since the original goal of the project was to maximize the number of cells that could be grown in a small area, various substrates were tested. The needed to promote the growth of cells cells that were 100% confluent, 100% differentiated, and had good morphology. In order to maximize

the total number of cells, hollow fiber membranes and stacks of flat plates in a small box were considered. The use of hollow fibers was of particular interest because of the large surface area they would provide for cell growth. Normally, cells are grown on cell culture-treated polystyrene however, polystyrene cannot be made into hollow fibers, so other materials were tested. Dr. Britt recommended that these trials initially take place on flat sheets, and rolling the sheets into hollow fibers could be done after attachment and viability on different surfaces was determined. The materials used for these trials were glass, polysulfone, and collagen-treated polystyrene.

Glass

The first substrate trial was done on glass petri dishes because glass has the potential to be made into small diameter capillaries, and is much easier to sterilize than other materials considered. Cells were grown for 12 days until contamination was observed, stopping the trial. The results of this trial are shown in Figure 12.

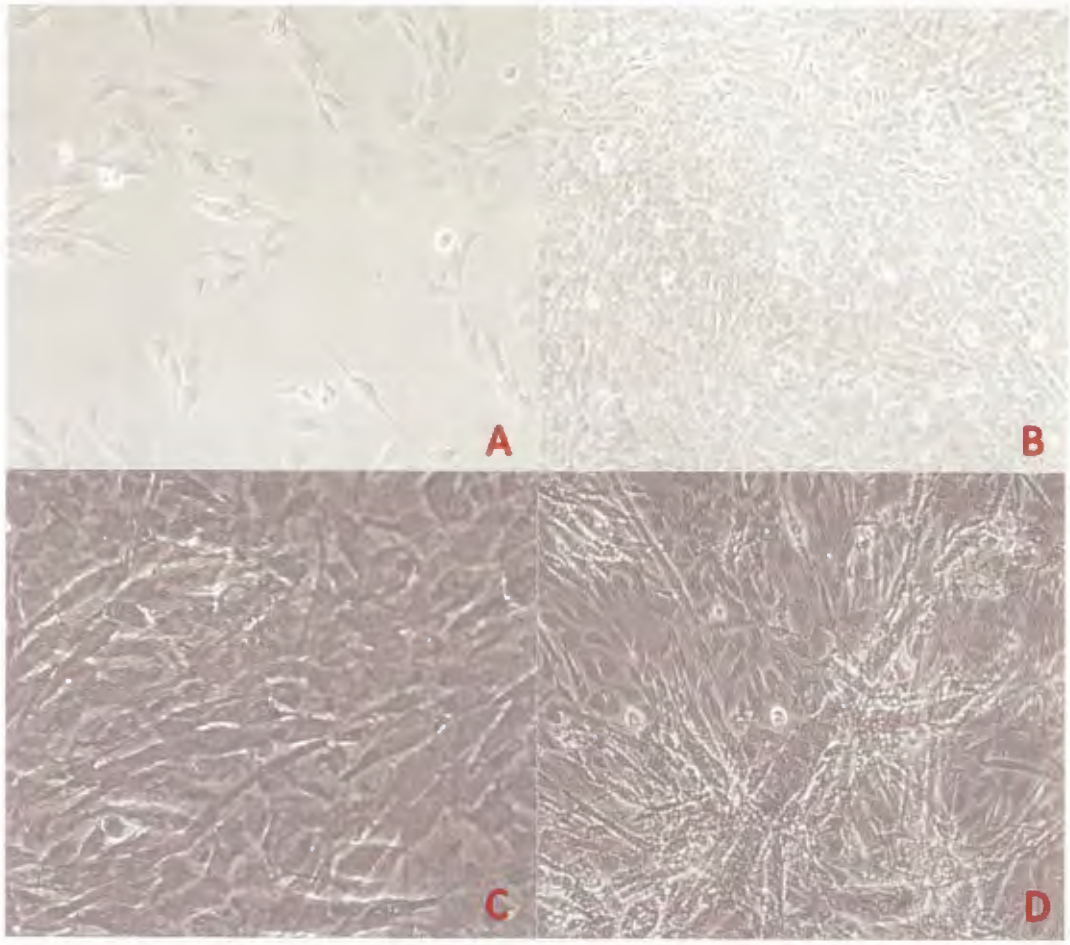

Figure 12. The progression of myoblast differentiation to muscle fibers grown on a glass petri dish. (A) Day 2, (B) Day 5, (C) Day 7, (D) Day 9. Scale = 100 μm.

Until the point when the cells became contaminated, growth on glass was successful. Cells grew and differentiated faster on glass than other substrates that were tested. Therefore, glass was considered as the substrate in the final design.

Polysulfone

Trials were done on polysulfone because it has the potential to be made into hollow fibers and is simple to fabricate. Polyethersulfone was also considered for the same reasons, but it was decided to use polysulfone because of it is cheaper and was already available.

In order to test cell growth on polysulfone, the polysulfone first had to be spun onto petri dishes. This was done according to the following procedure:

Materials

- PSP/PVP/DMAC
- dH_2O in two beakers
- Tweezers
- Aluminum Foil

Methods

1. Line spinner with aluminum foil to protect sides from spraying.
2. Place dish on spinner with vacuum attached and on.
3. Set speed and time on dials.
4. Press start and shield top to protect from spraying.
5. Remove dish and immediately dunk in dH_2O. Polymer will harden and turn white.
6. Allow film to air dry.
7. Sterilize with 70% ethanol under the hood.

Once the polysulfone had been spun onto petri dishes, it needed to be sterilized. This was a more difficult task than expected. At first, it was spun onto polystyrene petri dishes. Unfortunately, these could not be sterilized in the autoclave and never became completely sterile when soaked in bleach. The polysulfone was then spun onto glass petri dishes, which allowed it to be autoclaved, but the polymer shrunk during in the autoclave process, as shown in Figure 13.

Figure 13. Polysulfone shrunk in glass petri dish after sterilization in autoclave.

Although the polysulfone shrunk, a cell growth trial of on the polysulfone disk was still done. The results of this trial are shown in Figure 14.

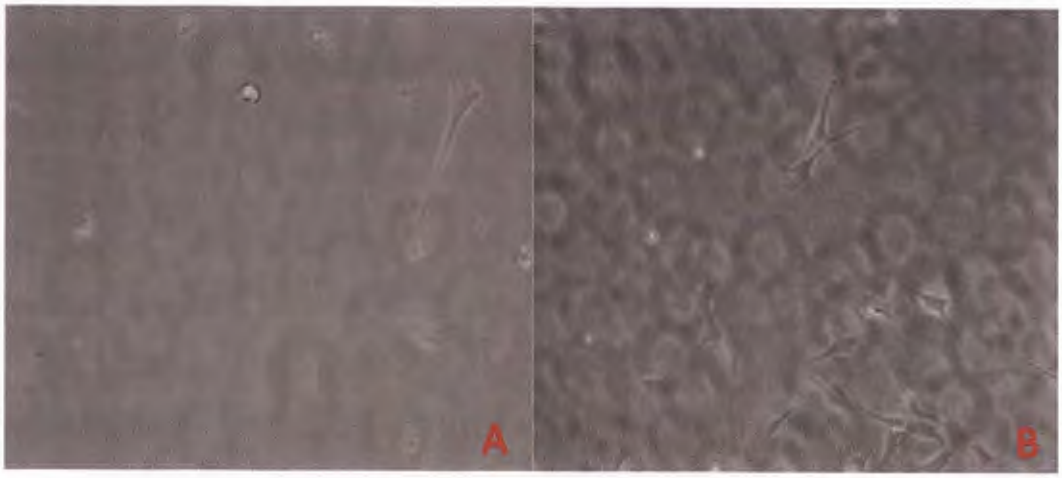

Figure 14. The lack of attachment and growth of cells on glass with polysulfone in the environment. (A) Day 2, (B) Day 5. Scale = 100 μm.

With the addition of the polysulfone disk in the dish, cells would not attach to the polysulfone or to the glass surfaces. Since polysulfone was difficult to sterilize, and did not promote cell growth, it was eliminated as a potential substrate for the final design.

Collagen

Since decellularized collagen is a common treatment used to stimulate cell growth, it was also considered as a potential substrate for the final design. In order to test this, T25 flasks were treated with Collagen I Rat Tail protein. The collagen treatment procedure is as follows:

Materials

- Cell Culture Flask

- Collagen I Rat Protein, Tail stock solution
- 20mM Acetic Acid
- PBH or DMEM 10% FBS media

Methods

1. Determine the volume needed for experimentation. (Stock Concentration: 3 mg/mL)
2. Dilute the collagen to 50 micrograms/mL in 20 mM acetic acid at the final volume needed. (Diluted to 50 micrograms/cm^2)
3. Add solution to plates or dishes at 5 microgram/square centimeter.
4. Incubate at room temperature for 1 hour.
5. Carefully aspirate solution from the well or dish.
6. Rinse dish three times with equal volumes of sterile 1X PBS or media to remove the acid.
7. Plates may be used immediately or air dried (store at 2-8C) for future use.

After the flasks had been treated with collagen, they were immediately seeded with C2C12 cells. The gradual differentiation of the myoblasts into muscle fibers over a 16-day period is shown in Figure 15.

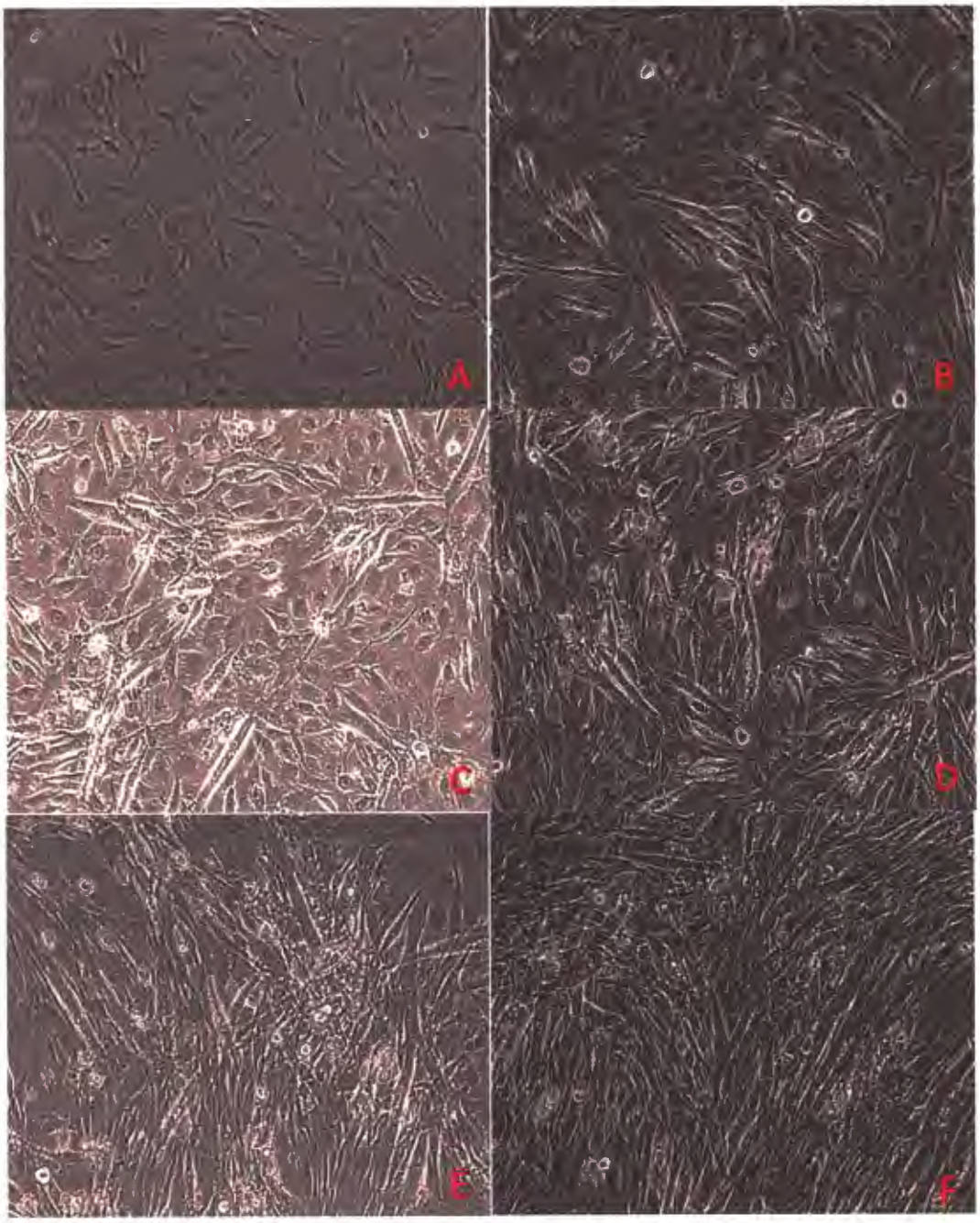

Figure 15. C2C12 cells grown on collagen treated petri dishes. (A) Day 2, (B) Day 5, (C) Day 9, (D) Day 12, (E) Day 14, (F) Day 16. Scale = 100 µm.

As Figure 15 shows, the cells grew and differentiated well, and did not experience contamination. Although it took the cells longer to grow on collagen than it took for them to grow on glass and polystyrene, collagen still promoted cell growth, and was considered as a substrate for the final design.

Overall Substrate Comparison

After the substrate tests were completed, the substrates were compared to each other to determine which would best support cell growth. This was determined based off of confluence, differentiation, and cell morphology. A comparison of confluence of cells over time on each substrate is shown in Figure 16.

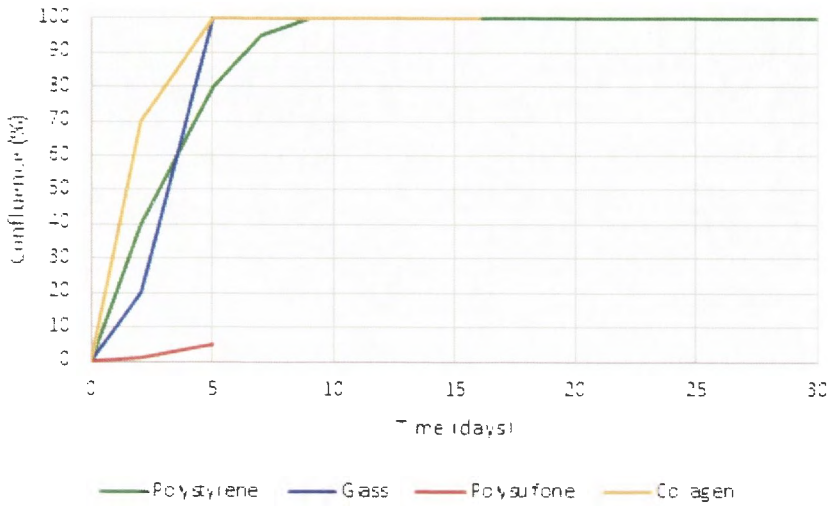

Figure 16. The confluence of polystyrene, glass, polysulfone, and collagen over different growth periods.

As seen in Figure 16, polystyrene, glass, and collagen all allowed the cells to grow to 100% confluence, meeting the requirement of the design, while polysulfone did not. Cells grown on polystyrene, glass, and collagen reached 100% confluence in approximately the same amount of time, indicating that none of these substrates were better than the others at producing 100% confluent cells. Differentiation of cells over time on each substrate, which was also an important consideration, is shown in Figure 17.

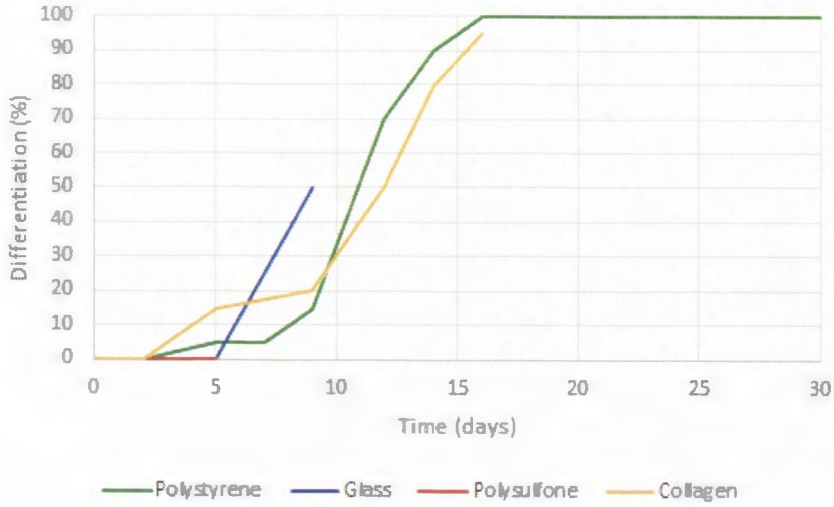

Figure 17. The differentiation of cells on polystyrene, glass, polysulfone, and collagen over different growth periods.

As seen in Figure 17, polystyrene was the only substrate that allowed the cells to differentiate completely. Most likely, cells grown on glass and collagen would have also allowed the cells to differentiate completely, but this information was not included in these trials. Once again, polysulfone was the only substrate that would not work for the final design. The final way in which substrates were compared is morphology. Images of the morphology of cells grown on the different substrates is shown below in Figure 18.

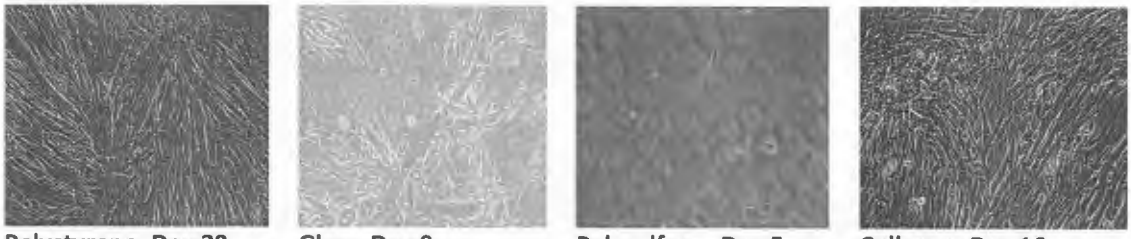

Polystyrene, Day 30
Morphology Score: 9/10

Glass, Day 9
Morphology Score: 7/10

Polysulfone, Day 5
Morphology Score: 2/10

Collagen, Day 16
Morphology Score: 9/10

Figure 18. Images of cells grown on polystyrene, glass, polysulfone, and collagen on the last day of the growth period.

By this point, the goal for the final design had changed significantly; hollow fiber membranes were no longer an important consideration, other tests had shown that radiation damage would not be significant enough for GeneChip analysis to detect. A Mann-Whitney U Test gave a p-value of 0.3702, indicating that the morphology of the cells grown on polystyrene was not significantly better than the morphology of cells grown on other substrates. However, the

polystyrene was much cheaper. Because of this, the data already collected in these cell culture trials were considered sufficient to decide that tissue-culture polystyrene would be the most appropriate substrate for the final design.

Cell Culture for Launch

Since it was determined that tissue culture polystyrene was the best substrate for cell growth, C2C12 cells were grown on polystyrene for a period of a period of two weeks prior to the launch date. On the day of the launch, two T12.5 cm^2 flasks of differentiated muscle cells filled completely with DMEM 2% FBS media, to eliminate shear forces on the cells. The cells exhibited good attachment, growth rate, and viability as seen in Figure 19.

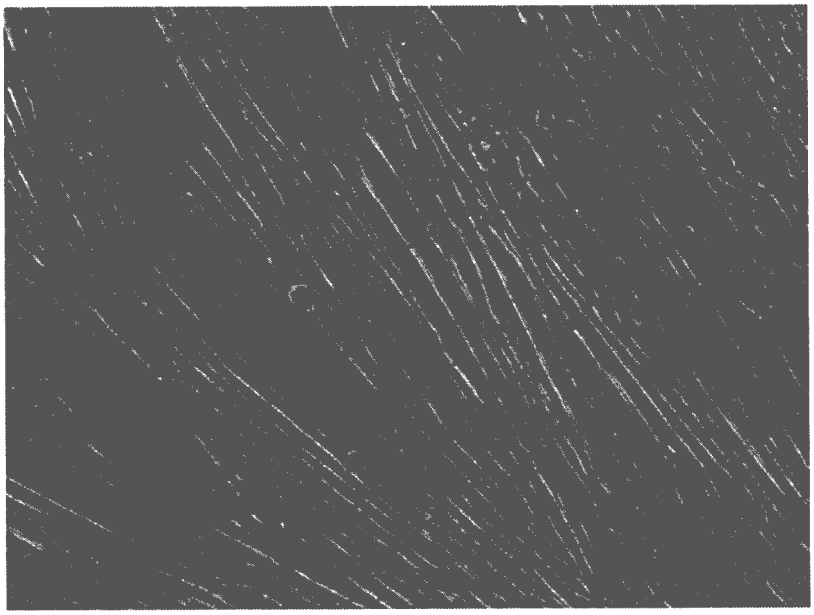

Figure 19. Experimental C2C12 cells grown in T12.5 flasks and differentiated using 2% FBS media before flight. Cells exhibited good attachment, growth rate, and viability. Scale = 100μm.

Two T12.5 cm^2 flasks of differentiated muscle cells were also filled completely with DMEM 2% FBS media then left in the incubator as a negative control. These cells exhibited good attachment, growth rate, and viability, and were selected for their similarity to the cells for launch as seen in Figure 20.

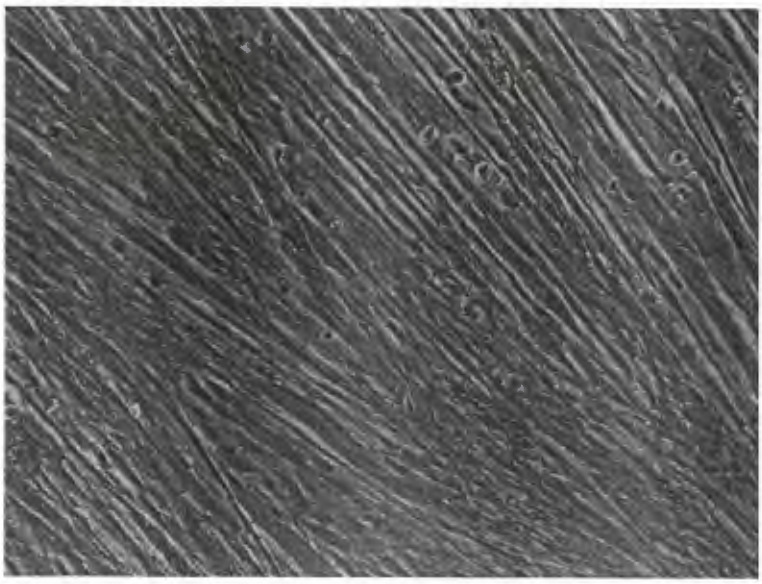

Figure 20. Negative control C2C12 cells grown in T12.5 flasks and differentiated using 2% FBS media before flight. Cells exhibited good attachment, growth rate, and viability. Scale = 100μm.

Additionally, after the flight, two T12.5 cm^2 flasks of muscle cells were differentiated and filled completely with DMEM 2% FBS media, then dropped from a height that would achieve the measured impact velocity from the flight as a positive control. These cells exhibited good attachment, growth rate, and viability as seen in Figure 21.

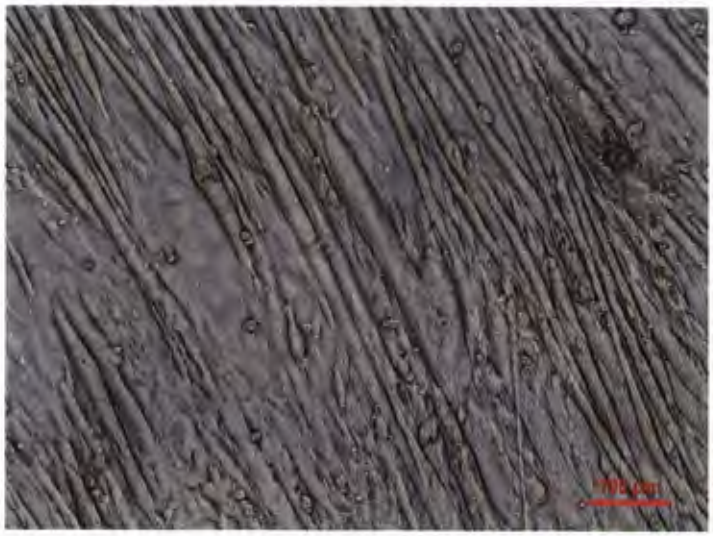

Figure 21. Positive control C2C12 cells grown in T12.5 flasks and differentiated using 2% FBS media before flight. Cells exhibited good attachment, growth rate, and viability. Scale = 100μm.

Overall, the experimental cell flasks had similar morphologies and viabilities as both the positive and negative control flasks indicating the payload successfully insulated the cells from flight and

landing forces as defined in the objective evaluation criteria. This made them appropriate selections for use in the final launch.

Radiation Testing

Since higher radiation levels are encountered in the upper atmosphere than on Earth's surface, radiation exposure testing was required to determine if further radiation shielding was necessary in the payload. Radiation dosage from the source was measured inside and outside the Mylar shielded payload; there was no difference in the gamma radiation measured indicating that gamma radiation was not shielded by the payload as seen in Figure 22.

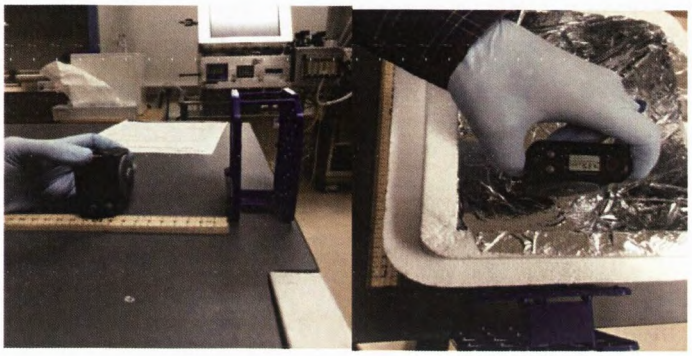

Figure 22. Left: Calibration of radiation dosage. Right: Measurement of radiation passing through Mylar shielding.

The cell flasks within the payload were shielded from both alpha and beta particles with an aluminized mylar lining on the interior of the container. To measure radiative effects, cells were exposed to doses of radiation comparable to those encountered at 20 km above the Earth's surface (Friedberg 2011) according to the following procedure:

Materials

- Differentiated cells
- Mylar shielded payload
- Cesium 137 disks
- Geiger counter
- One inch thick lead shield

Methods

1. Place two flasks of differentiated cells on top of four Cs 137 disks inside the incubator
2. Place one flask of differentiated cells within 10 cm of the Cs 137 disks with a lead shield between the flasks and the radiation source
3. Place one flask of differentiated cells in a separate incubator as a control
4. Incubate for 24 hours

The experimental setup included four flasks of differentiated cells, two placed on top of four Cesium 137 disks, one shielded from radiation with a thick lead slab, and one control in a separate incubator as shown in Figure 23.

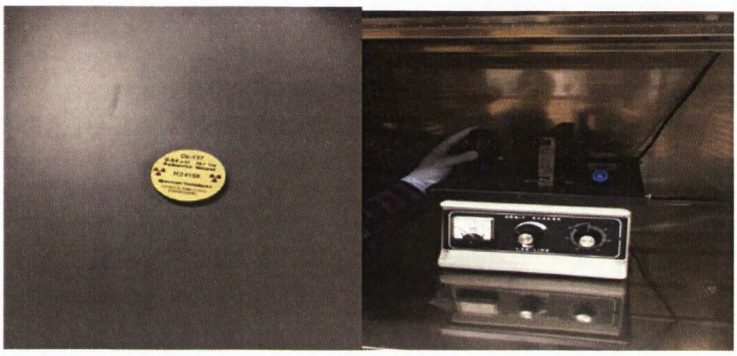

Figure 23. Left: Cesium 137 disk used to provide radiation dose. Right: Experimental setup as described in Methods with two flasks on top of Cs disks and one flask shielded with a lead slab. Not pictured: Control flask.

After 24 hours of incubation, there were no morphology changes or significant viability differences between experimental and control flasks as seen in Table 6. Viability was measured using a Trypan Blue assay.

Table 6. Cell viability following 24 hours of incubation. Radiated flasks were exposed to a calculated 4 μSV/hr, the control flask was incubated without added radiation, and the shielded flask was shielded from additional radiation with a one inch thick lead slab.

	Viability
Control	92%
Radiated Flask 1	97%
Radiated Flask 2	97%

	Viability
Shielded Flask	94%

It was decided not to include additional radiation shielding in the payload design since there were no significant differences in viability or morphology between exposed and control cell flasks.

pH Testing

To ensure the payload could provide an environment suitable for at least 50% cell viability after the flight, cells were enclosed in a filled T25 cm^2 flask for a period of 24 hours. This tested whether cells could survive without fresh media, oxygen, and carbon dioxide. After 24 hours, no visible changes were seen in the cells. Results of this test are shown below in Figure 24.

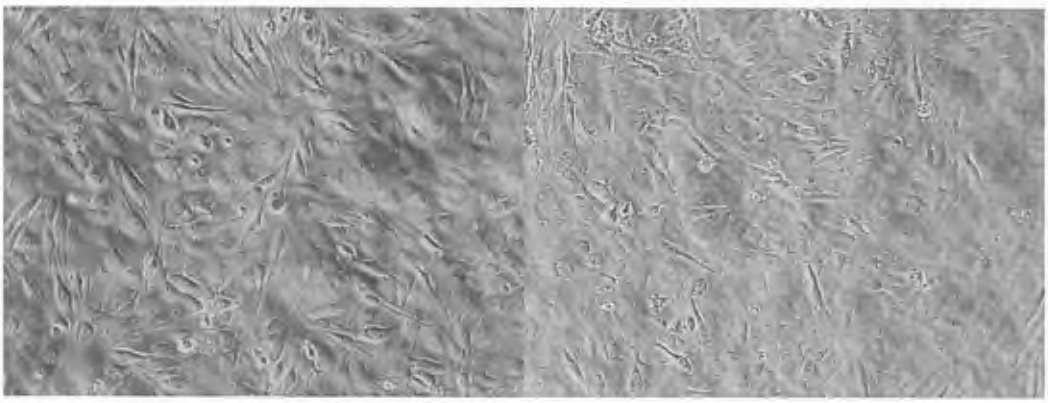

Figure 24. Left: Early differentiated C2C12 cells. Right: Early differentiated C2C12 cells after 24 hours with no nutrients, oxygen, or CO_2 available.

The cells showed no visible changes throughout the trial and remained healthy after they were returned to the incubator. The pH at the beginning of the trial was 8.2, and after 24 hours it had dropped to 7.5. The pH was not measured at intervals during the trial because opening the flask to test the pH would introduce additional oxygen and carbon dioxide into the flask. These results indicated that a gas exchange mechanism would not be necessary for a flight of this length.

Protective Casing Design

Because the payload was likely to experience relatively high impact forces, a protective casing was developed to surround the payload. Impact speed was predicted to be 17 m/s based on the results of similar balloon launches. Designs were developed following a consultation with CRSA, an architecture firm specializing in blast proof construction for the US military. For each iteration, the design was constructed then dropped from a height to simulate impact speed with the payload centered within the casing.

The first iteration of the design included fiberglass rods held together with custom wood joints at each vertex. This design was improved to use carbon fiber rods to reduce the weight. A schematic of this design is shown in Figure 25.

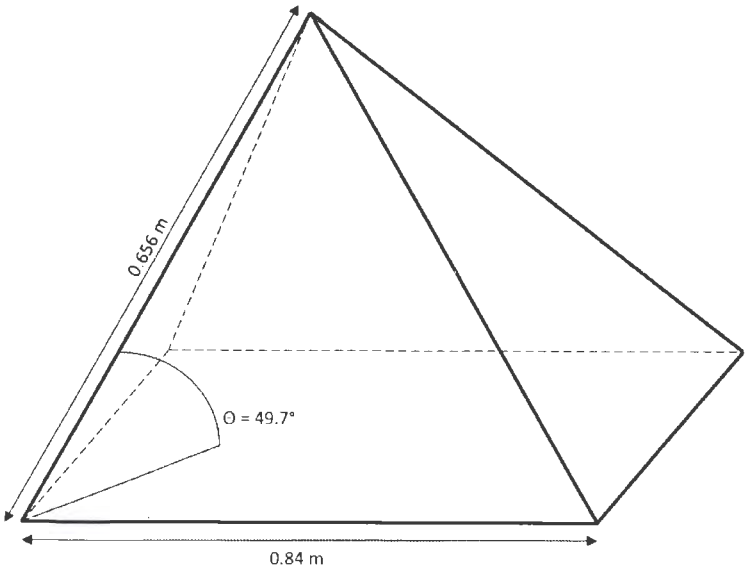

Figure 25. Schematic of square pyramid carbon fiber protective casing. The payload would be suspended within the pyramid.

To provide maximal impact cushioning, the pyramid would need to break which was most likely to happen if it landed on a vertex. Upon landing and breaking, the pyramid would redistribute the shock throughout the carbon fiber rods and provide some protection for the suspended payload. With an approximated weight of 450 grams, there was a moderate probability that the pyramid would not land on a vertex and therefore not provide optimal cushioning for the payload.

The next iteration of the protective casing design included many small, frangible Styrofoam cubes surrounding the payload. A schematic of this design is shown in Figure 26.

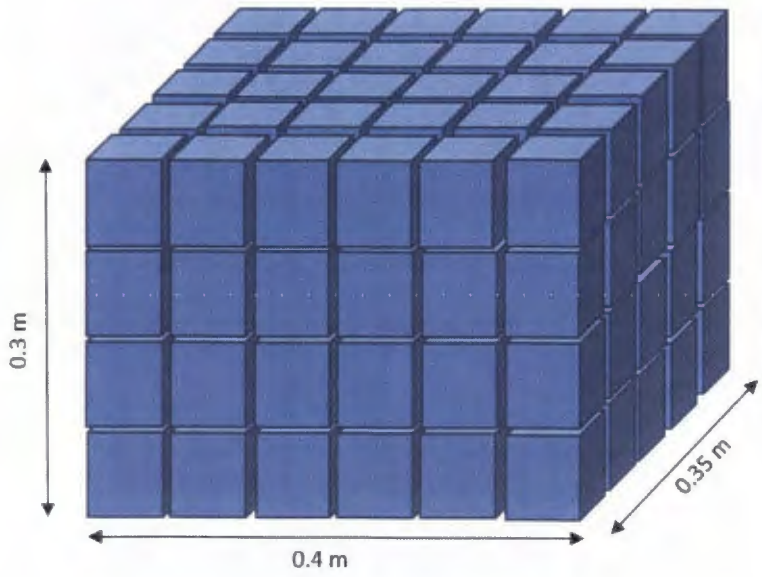

Figure 26. Schematic of frangible Styrofoam cube matrix designed to protect the payload. The payload would be positioned in the center of the cube matrix.

The frangible Styrofoam cube matrix provided a uniform impact surface, giving a probability equal to 1 that the design would protect the payload to the maximum of it's ability. The design weighed approximately 600 grams. This iteration of the casing was rejected due to it's complex fabrication and difficulty of consistent reconstruction.

The final iteration of the design improved upon the frangible cube matrix by exchanging custom built Styrofoam cubes with large Styrofoam packaging peanuts packed closely within a plastic bag reinforced with nylon fiber. Using a nylon fiber reinforced bag reduced the probability of breakage on landing however, biodegradable peanuts were used to minimize environmental impacts in the event of spillage. The payload was packed in the center of the bag and surrounded completely by peanuts as seen in Figure 27.

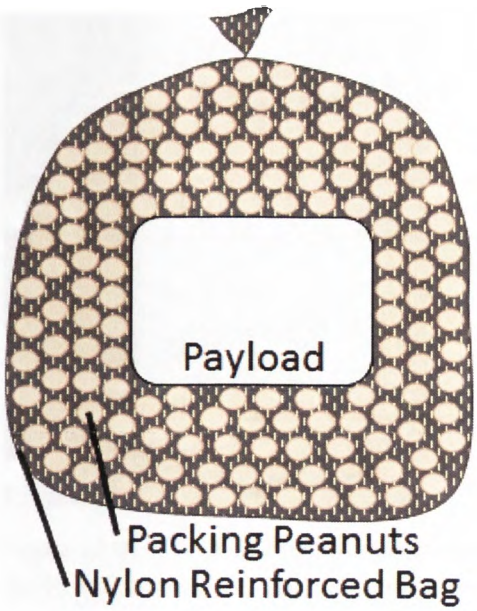

Figure 27. Schematic of nylon reinforced plastic bag (lines on bag) containing the payload surrounded by biodegradable packaging peanuts.

The nylon reinforced bag provided a relatively uniform surface for impact giving a low probability of failure. The packaging peanuts provided similar impact absorption capabilities as the frangible cube matrix without the inconsistency in fabrication. The system weighed approximately 550 grams and was chosen as the final design to protect the payload.

Cell Drop Test

To determine if the payload could effectively insulate cells from flight and landing forces, the payload was attached to a 5ft diameter nylon parachute and cushioned inside a frangible container to minimize impact forces felt by the cells. The predicted impact speed was 6.7 m/s (approximately 15 mph) based on measurements taken by the United Kingdom HabHub society. A drop height of 2.6 meters was calculated using potential and kinetic energy formulas with a mass of 2.3 kg. One T25 cm2 flasks was completely filled with media to prevent shear forces on the cells, then surrounded with packaging peanuts in a styrofoam container as seen in Figure 28.

Figure 28. A flask of differentiated cells was filled with media then packed in packaging peanuts and dropped from 2.6 m to simulate impact speed.

The container fell for 1.4 seconds before impacting with the concrete floor. The flask was emptied and the media was centrifuged to collect dislodged cells. The flask was returned to the incubator with fresh media. There were no cells growing in the flask 24 hours following the drop test.

To improve the probability of cell survival in the payload, a suspension method was tested. Two T12.5 cm^2 flasks of differentiated C2C12 cells were filled completely with media and connected together using rubber bands then suspended in the payload with nylon as seen in Figure 29. The drop test followed the same protocols outlined in the failed test above.

Figure 29. Two flasks of differentiated cells were suspended in the payload and dropped from a height of 2.6 meters to simulate landing impact.

The payload fell for 1.1 seconds and impacted with the cement floor with a force of 22.54 Newtons. Cell morphology before and after the drop is shown in Figure 31. Viability after the test was measured by removing the media from the flask, centrifuging, resuspending the cell pellet and counting the cells with Trypan blue®. On average, there were 2 dead cells/mm^2 on the hemocytometer indicating a high viability. Images of this are shown in Figure 30.

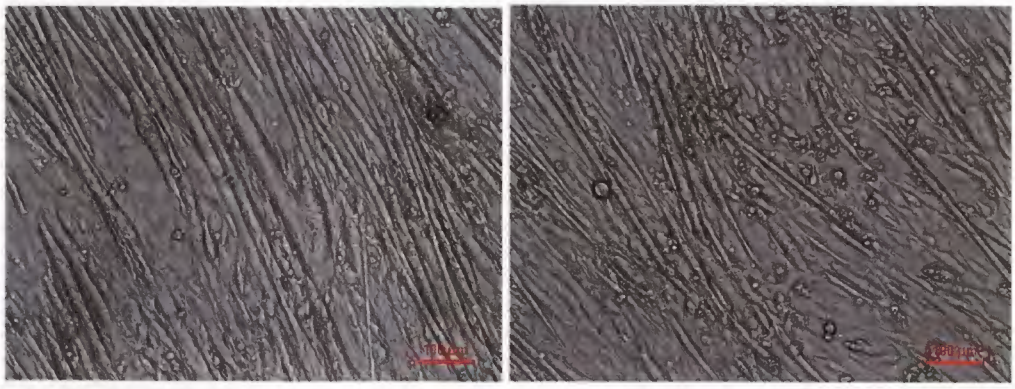

Figure 30. Left: Differentiated cells before dropping in payload from 2.6 meters. Right: Differentiated cells after dropping payload from 2.6 meters. Scale = 100 μm.

The post-drop cells had slightly spherical morphology in some areas indicating cell detachment. 2.5 ml of DMEM-F12 2% FBS media was added to the flask post-drop which was then incubated at 37°C with 5% CO_2.

Microcontroller Design and Programming

In order to make sure the temperature sensors and heating pads functioned correctly, it was necessary to use a microcontroller. Initially, it was expected that the components could be easily attached and a simple code could be written, but the actual process was more difficult.

In the first iteration of the design, the temperature sensors and the heating pads were connected directly to the output from the microcontroller. After initial tests with this design, it was discovered that the internal temperature sensor was working correctly, but the external temperature sensor was not working, and the heating pads were not warming. Further research revealed that the external temperature sensor needed a 4.7 kΩ pull-up resistor to function correctly, and the heating pads needed approximately 750 mA of current to function properly, instead of the 20 mA being supplied by the Arduino.

The second iteration of the design fixed the issue with the external temperature sensor, but did not fix the problem with the heating pads. Including the pull-up resistor allowed the external temperature sensor to function properly. A closer look at the specifications of batteries revealed that standard 9V batteries would not be able to output enough current. Energizer *Ultimate Lithium* batteries were selected to increase the total amperage to 1000 mA. Three batteries were connected together in parallel to ensure that the heating pads would work for the duration of the flight. Connecting the batteries in series would have increased the current and allowed the heating pads to heat up more quickly, but this would have also caused the current to exceed the maximum acceptable for the batteries. Since the selected batteries were relatively expensive, a wall adapter was purchased so the design could be tested without using unnecessary battery power. In addition to the extra battery, an op-amp was connected so the voltage from the batteries would match the voltage from the Arduino. However, the op-amp did not function properly. It overheated quickly any time power was connected to the Arduino, and the heating pads did not heat properly when it was in use. Replacing the op-amp with another one from the package did not solve the problem. It was suspected that the part was inadequate for the job, despite the fact that the manufacturer claimed it had a maximum of 36V.

Since the op-amp did not work properly, it was replaced with a transistor in the final design. This was incorporated successfully into the microcontroller design. The heating pad worked well, although it didn't get as warm as expected. To fix this, an additional 1.5V (D) battery connected in series was considered to increase the voltage. However, this would have added extra weight to the design, so a freezer test was run without this addition, and it was determined that the cells

could stay warm enough without the extra voltage to power the heating pads. A schematic of the final design is shown in Figure 31

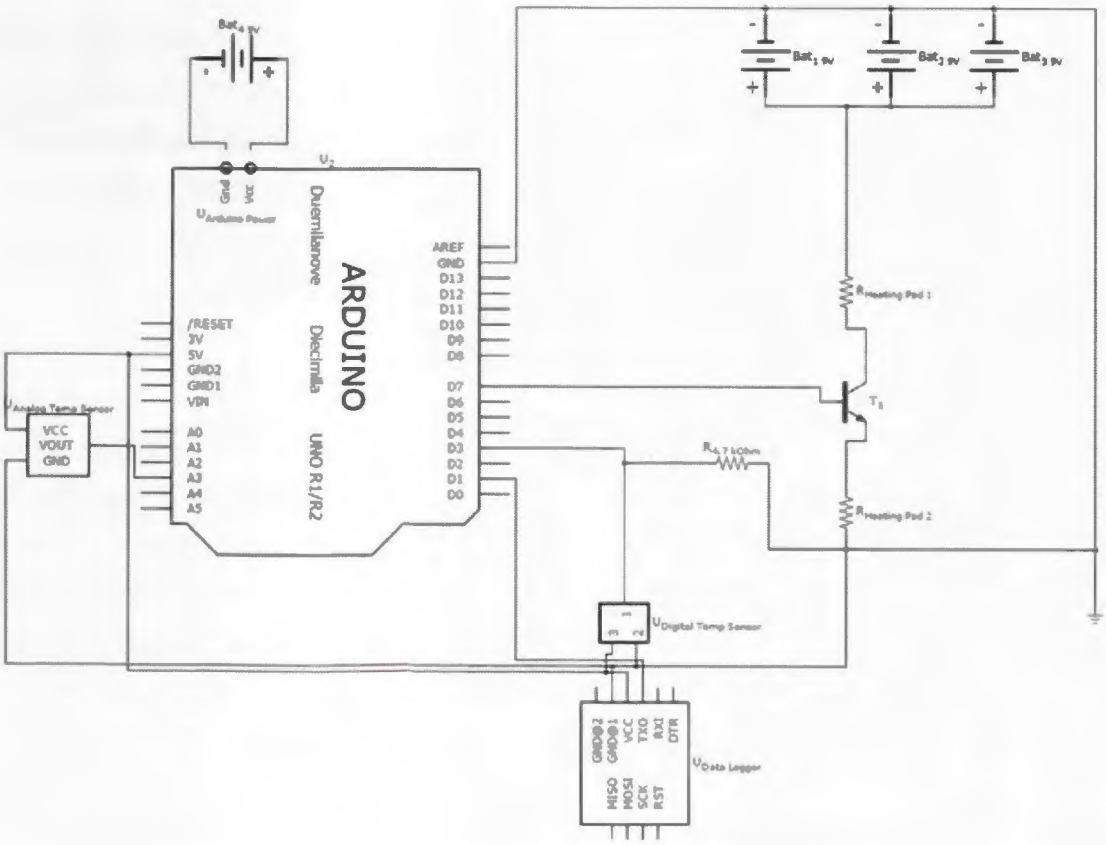

Figure 31. A schematic of the microcontroller and the attached sensors.

The code used to for the microcontroller is as follows:

```
#include <OneWire.h>

int analogTempPin = 3; //FIXME: what pin is it lol
int heaterPin = 7; //FIXME: what piiiiin
int DS18S20_Pin = 3; //DS18S20 Signal pin on digital 5
char tmpstring[10];
int timeCounter = 0;
```

```
int logTicker = 0;

OneWire ds(DS18S20_Pin);  // on digital pin 2

void setup() {
 // put your setup code here, to run once:
 Serial.begin(9600);
 //pinMode(DS18S20_Pin,INPUT_PULLUP);
 pinMode(heaterPin, OUTPUT);
 Serial.println("Minute,Inside,Outside");
}

void loop() {
checkTemps(logTicker);
delay(1000);
logTicker++;
if (logTicker >= 7) {
 logTicker = 1;
}
}

void checkTemps(int cycleNumber) {
 int innerTemp = (int) getInsideTemp();
 if ((cycleNumber % 6) == 0) {
   logTemps(innerTemp);
 }
 if (innerTemp >= 39) {
   digitalWrite(heaterPin,LOW);
 }
 if (innerTemp <= 35) {
   digitalWrite(heaterPin,HIGH);
```

```
 }
 return;
}
void logTemps(int inTemp){
int outTemp = (int) getOutsideTemp();
Serial.print(timeCounter++);
Serial.print(",");
Serial.print(inTemp);
Serial.print(",");
Serial.println(outTemp);
return;
}

float getInsideTemp() {
 int rawvoltage= analogRead(analogTempPin);
 float volts = rawvoltage/205.0;
 float celsiustemp= 100.0 * volts - 50;
return celsiustemp;
}

float getOutsideTemp(){
 //returns the temperature from one DS18S20 in DEG Celsius

 byte data[12];
 byte addr[8];

 if ( !ds.search(addr)) {
     //no more sensors on chain, reset search
     ds.reset_search();
     Serial.println("No stupid thing found");
     return -1000;
```

```
}

if ( OneWire::crc8( addr, 7) != addr[7]) {
    Serial.println("CRC is not valid!");
    return -1000;
}

if ( addr[0] != 0x10 && addr[0] != 0x28) {
    Serial.print("Device is not recognized");
    return -1000;
}

ds.reset();
ds.select(addr);
ds.write(0x44,1); // start conversion, with parasite power on at the
end

byte present = ds.reset();
ds.select(addr);
ds.write(0xBE); // Read Scratchpad

for (int i = 0; i < 9; i++) { // we need 9 bytes
  data[i] = ds.read();
}

ds.reset_search();

byte MSB = data[1];
byte LSB = data[0];

float tempRead = ((MSB << 8) | LSB); //using two's compliment
float TemperatureSum = tempRead / 16;
```

```
 return TemperatureSum;
}
```

Tracking System Design

Because the payload needed to be recovered for analysis, it was necessary to design a tracking system. High-altitude balloons are generally tracked using either GPS or APRS tracking. GPS tracking is generally very effective, but most transmitters do not work above 60,000 ft. APRS tracking sends signals to radio towers, and HAM radio operators decode the signal. In the final design of the tracking system, a combination of GPS and APRS was used. A special GPS receiver was used to transmit the location of the balloon from satellites and a radio transmitter sent the position to the APRS network.

High Altitude Flight Test

The payload was launched on Saturday, November 5, 2016 at 7:35 am from an open area outside Howell, UT. The launch location was determined using HabHub's Flight Prediction software to determine the most likely landing site. The software takes balloon size, gas volume, launch altitude and time, local weather, and payload weight into account. Predictions were run every half hour beginning at 5:00 am on the day of the launch. The final prediction is shown in Figure 32.

Figure 32. Flight prediction made by HabHub's software. The red dot denotes the launch site, the orange dot denotes the predicted balloon burst location, and the green dot denotes the predicted landing site. Burst altitude was predicted using the burst calculator function. The software takes balloon size, gas volume, launch altitude and time, local weather, and payload weight into account.

The payload was prepared and sealed in the lab prior to the launch. The tracking system and balloon were both prepared at the launch site according to the following procedures.

Payload Preparation

1. Completely fill two 12.5 cm2 flasks of differentiated C2C12 myoblasts with warmed DMEM F-12 with 10% FBS.
2. Connect microcontroller to batteries to begin data collection.
3. Firmly attach microcontroller, batteries, geiger counter, and hot hand warmers to bottom and sides of the payload container with duct tape.
4. Cut two pieces of nylons (tube shape) approximately four inches long to hold the cell flasks.
5. Make a hole, approximately 0.24" in diameter, in one piece of nylon.
6. Connect the two cell flasks together with elastic bands and insert them into one piece of nylon.
7. Use small rubber bands to secure the flasks in place on either side.
8. Insert the enclosed flasks into the second piece of nylon through the small hole so that the connected flasks are centered within both pieces of nylon.
9. Use small rubber bands to secure the flasks in place on either side.
10. Stretch the nylon ends to the side of the payload container and attach firmly with an industrial stapler.
11. Place one heating pad on top of the suspended cell flasks and one below. Attach with tape.
12. Extend the external temperature sensor outside the payload container.
13. Attach the lid to the container firmly with duct tape.
14. Enclose the payload within the protective casing by surrounding it the payload completely with Styrofoam peanuts then zip tying the bag closed.
15. Wrap the zip ties with duct tape to prevent snagging.

16. Attach a label to the payload with contact information.

17. Attach the top of the payload to the bottom of the tracking system using mason line and zip ties.

Tracking System Preparation

1. Power on and test both the GPS and radio transmitters.

2. Attach the GPS and radio transmitters firmly to the side of the container.

3. Connect the radio antenna to the radio transmitter and leave the antenna outside the container.

4. Close the container and duct tape the lid closed.

5. Attach the bottom of the parachute to the top of the tracking system with mason line and zip ties.

Balloon Preparation

The balloon was inflated with the help of Stanley Wellard, a retired engineer from Space Dynamics Lab and part of the Cache Valley Ham Radio Society.

1. Spread a large, clean tarp on a flat surface.

2. Wearing latex or nitrile gloves, carefully unpack the balloon without letting it touch the ground.

3. Have two people hold the neck of the balloon as it's being inflated, the remaining people should hold the body of the balloon to ensure it doesn't touch the ground.

4. Add enough helium so that the lift force is in equilibrium with the payload weight. This was tested with a water bottle filled to be the same weight as the payload.

5. Attach the balloon to the parachute by folding the neck in half around a paracord loop and zip tying the balloon closed as seen in Figure 33.

6. Wrap the zip ties with duct tape to prevent snagging.

Figure 33. Stanley Wellard attaching the balloon to the parachute by threading the neck of the balloon through a paracord loop on the parachute. The neck of the balloon was folded in half, zip tied closed, and wrapped in duct tape.

All individual components were connected to each other using mason line, zip ties, and duct tape in the following order: balloon, parachute, tracking system, test payload as seen in Figure 34.

Figure 34. The final layout of the flight with the balloon attached to the parachute (note: the hula hoop prevents the strings from tangling during flight) which was attached to the tracking system which was attached to the experimental payload.

The final weight of the payload system was 2.7 kg (5.9 lb) including the parachute, tracking system, and experimental payload, meeting the objective of a payload less than six pounds previously defined.

Launch Results

The balloon carried the payload to a maximum altitude of 28, 540 m (93,611 ft) with a total flight time of 1 hour and 51 minutes. The payload landed in Fielding, UT (Lat: 41.80814 Long: -112.103), approximately 7.3 km (4.5 miles) short of the predicted landing site. The flight path is shown in Figure 35. Flight speed and altitude are shown in Figures 36 and 37, respectively.

Figure 35. Flight path data from aprs.fi, the software relay for the radio and GPS transmitters. The orange dot denotes balloon burst and the red hot air balloon icon denotes the landing location.

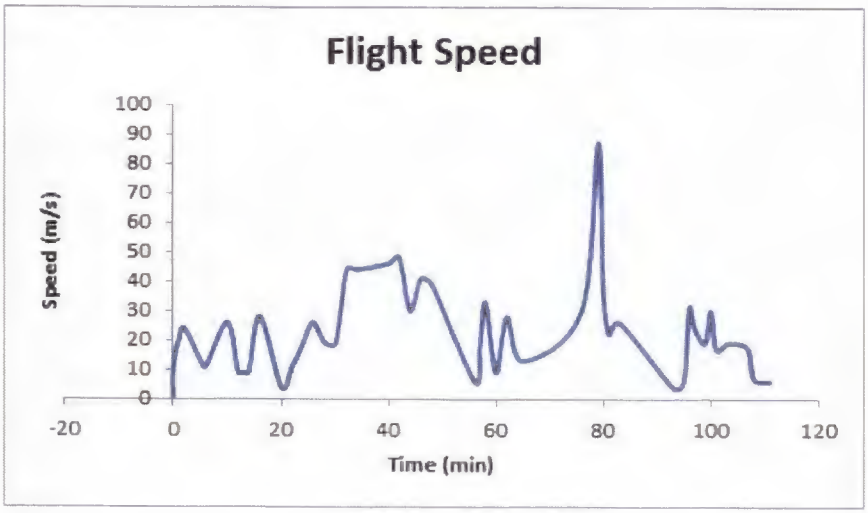

Figure 36. Speed vs time graph of payload. The maximum speed was 87 m/s at the time of burst.

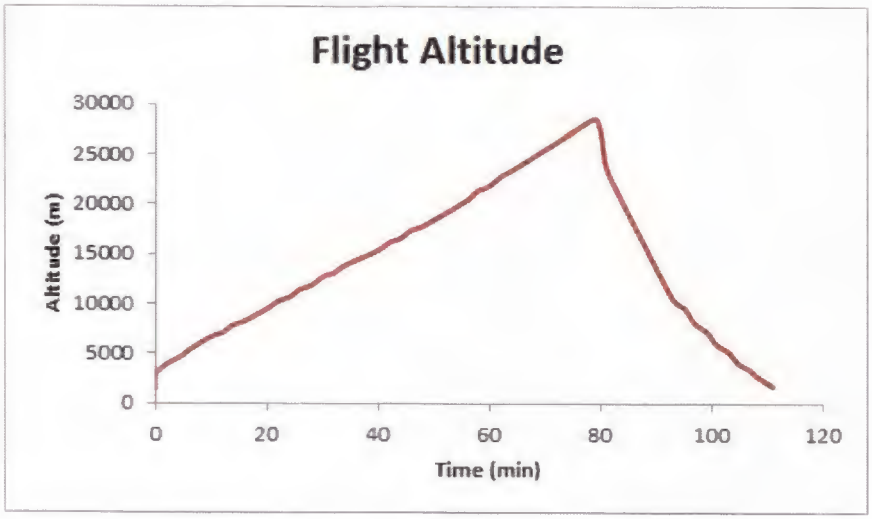

Figure 37. Altitude vs time graph of payload.

Cells proved to survive the entire flight and continued to thrive up to a week after the flight. Images of cells immediately before and after launch are shown in Figure 38.

Figure 38. (A) C2C12 cells pre launch. (B) C2C12 cells post launch.

Analysis of launch cells were conducted immediately after the launch and 7 days later. The results of this analysis are shown in Table 7. Launch B and Positive Control A were passaged and counted for viability and replaced in new flasks, while Launch A and Positive Control B were left alone and placed back in the incubator. After 7 days, all launch cells and controls were passaged and tested for viability. Launch flasks were completely filled with media and the positive control flasks were also completely filled with media, but left on the ground in an incubator. Negative controls contained 2.5 mL of media and stayed in the same incubator during flight.

Table 7. Cell viability results after payload flight. Both Launch A and Positive Control B flasks were allowed to grow uninterrupted for 7 days post-launch. Viability for Launch B and Positive Control A flasks was analyzed immediately, then reseeded for 7 days of growth. CT = contamination

	Viability (%)	
	Immediately Post-Launch	7 Days Post-Launch
Launch A	--	88
Launch B	89	93
Positive Control A	91	CT
Positive Control B	--	88
Negative Control	--	78

Final Design Review

The final design of the payload included two T12.5 cm^2 flasks connected together and suspended by nylon in an insulated container as seen in Figure 16. The styrofoam container was wrapped in aluminized mylar on the inside to shield both flasks from alpha and beta particles as well as provide insulation to reduce heat loss to the environment. A cardboard layer was attached to the mylar to provide better attachment of the nylons, then covered in a secondary layer of mylar. Both layers of mylar and the layer of cardboard was attached using a 3M Styrofoam safe spray adhesive. The nylon suspension system attached diagonally to the top and bottom of the interior to provide maximum force absorption on impact. The Geiger counter and microcontroller were attached to the bottom and sides of the insulated container. The heating pads sandwiched the cell flasks between them. The external temperature sensor connected to the microcontroller and exited the container through a small hole to the environment. A schematic of the final design is included in Figure 39.

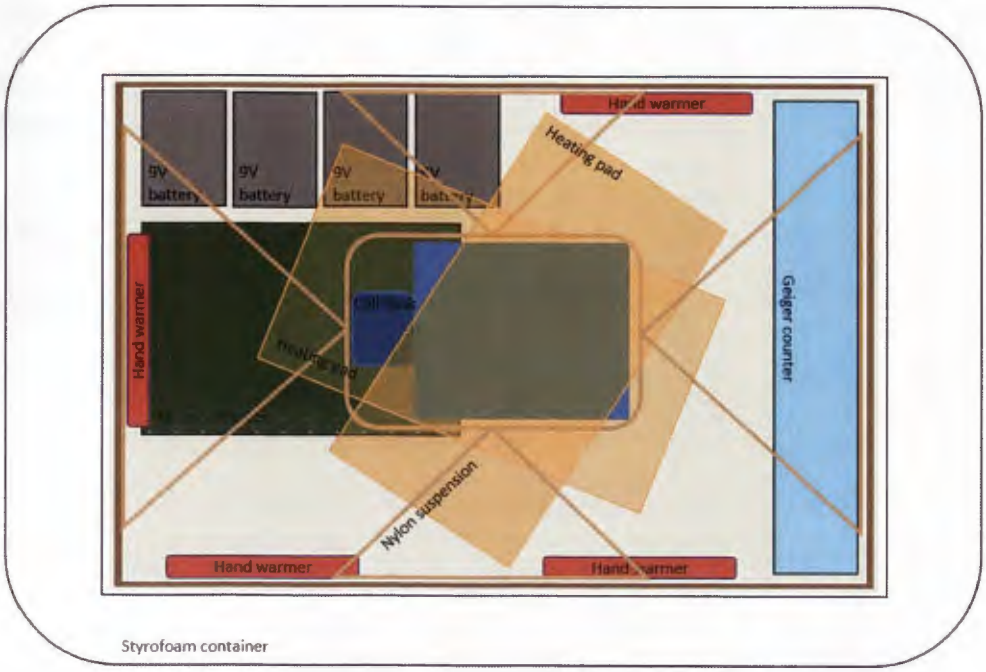

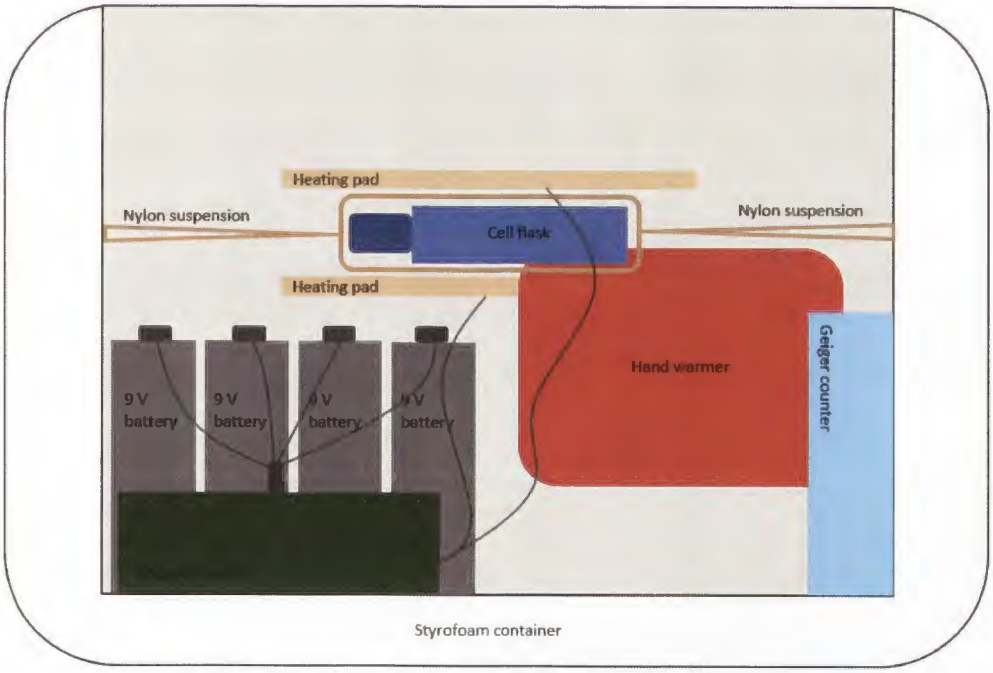

Figure 39. A schematic of the final payload design including the microcontroller and batteries, hand warmers, heating pads, Geiger counter, and suspended cells. Above: top view of payload. Below: side view of payload.

The individual components of the payload were placed inside to minimize the probability of the cell flask coming into contact with them and potentially disrupting cell adhesion. Each component was firmly attached to the bottom or sides of the payload using duct tape to reduce the probability damage during the flight.

Materials Used

Microcontroller and sensors

- Microcontroller
    - Brand: Arduino
    - Type: Uno R3
    - Model number: A000066
- Heating pads
    - Brand: Sparkfun
    - Model number: COM-11288
- Exterior temperature sensor
    - Brand: Sparkfun
    - Model number: SEN-11050
- Interior temperature sensor
    - Brand: Sparkfun
    - Model number: SEN-10988
- Data logger
    - Brand: Sparkfun
    - Model number: DEV-13712

Microcontroller fabrication

- 9V battery clip connector
    - Brand: ElectroAntics
    - ASIN: B00GN7VIZA
- Electrical wire
    - Brand: Sparkfun
    - Model number: PRT-08022
- Solder wick

    - Brand: Sparkfun
    - Model number: TOL-09327
- Microcontroller protoshield
    - Brand: Arduino by Sparkfun
    - Model number: DEV-11665
- 9V to barrel jack adaptor
    - Brand: Sparkfun
    - Model number: PRT-09518
- Arduino stackable header kit
    - Brand: Sparkfun
    - Model number: PRT-11417
- Lead free solder
    - Brand: Sparkfun
    - Model number: TOL-09163
- Power adapter
    - Brand: BINZET
    - ASIN: B00PJZQDDO
- Amplifier driver integrated circuit
    - Brand: uxcell
    - Part number: a14060700ux0171
    - UNSPSC code: 32111603
- Batteries
    - Brand: Energizer *Ultimate Lithium*
    - Model number: EVEL522BP2
    - ASIN: B01684J7P0

Flight materials

- Cordage
    - Brand: T.W. Evans
    - Model number: 11-193
    - ASIN: B000W8F7FS
- Balloon

    - Brand: Kaymont
    - Type: 1200 gram 30 ft. diameter
    - Model number: 122071494719
- Helium 300 L
    - Supplier: USU Lab Gas
- Spray adhesive
    - Brand: 3M
    - Type: Foam Fast 74
    - Manufacturer number: 62495049504
- Mylar blanket
    - Brand: Mylar
    - UNSPSC code: 42171701
- Hand warmers
    - Brand: HotHands
    - ASIN code: B01KKHZMLE
- Tracking antenna
    - Brand: Micro-Trak
    - Model number: V6
    - Seller: byonics.com
- Geiger counter
    - Brand: GQ
    - Model number: GMC-300E Plus
    - UNSPSC code: 26142300
    - ASIN number: B008GRTSV6

Cell culture materials

- Culture flasks
    - Brand: Corning
    - Type: 12.5 plug-seal
    - Manufacturer's number: 353018
- Growth media
    - Brand: HyClone

- Type: DMEM F12
- Manufacturer's number: SH30023-FSPM

Final Design

The overall design of the payload was able to successfully insulate cells from launch, flight, and landing forces by suspending the cell flasks in nylon mesh above the sensors. The nylon mesh was attached to the sides of the container using industrial staples. Electrical and duct tape was used to attach the microcontroller, batteries, hand warmers, and Geiger counter to the container walls. Painter's tape was used to attach the heating pads to the surface of the cell flasks as seen in Figure 40.

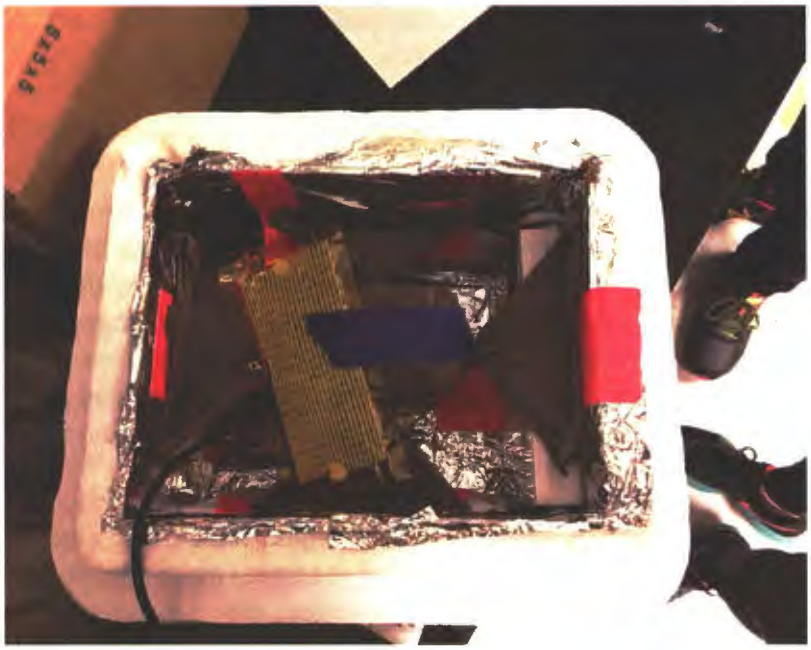

Figure 40. Final payload design to carry cells into the stratosphere with minimal damage. Two T12.5 cm flasks were attached together and suspended within the styrofoam container by nylon. The container was insulated with aluminized mylar on the inside to shield alpha and beta particles as well as provide heating insulation.

The cells were packed in the payload at 6:30 am on November 5, 2016 then returned to the lab after flight at 12:20 pm where they were analyzed. Viability assays were done on one of the two experimental flasks and one of the two control flasks. The trypsinized cells were then reseeded and incubated for one week. The remaining experimental and control flasks were filled with fresh media and incubated for one week. A positive control flask was dropped from a height to simulate the measured impact speed of the experimental flasks, following which a viability assay was performed. Results of these assays are summarized in Table 8.

Table 8. Summary table of viability assays performed on experimental, positive control, and negative control cell flasks following flight. CT = contamination.

	Viability (%)	
	Immediately Post-Launch	7 Days Post-Launch
Launch A	--	88
Launch B	89	93
Positive Control A	91	CT
Positive Control B	--	88
Negative Control	--	78

Based on these results and data recorded by the microcontroller, the overall design met the evaluation criteria defined at the beginning of this report. It reached a maximum altitude of 28.5 km, had a total flight time of 1 hour and 51 minutes, weighed 5.9 pounds, was easily recovered with real time tracking, and maintained an interior temperature between 27°C and 39°C.

Conclusions

The final design of the high-altitude payload met each objective through the use of feedback loops on a microcontroller, lightweight materials, a protective outer shell, a shock absorbing inner suspension system, and real time tracking throughout the flight. This work could provide a low-cost method of testing delicate biological samples hardiness during flight before subjecting those samples to costly space experiments. In addition to preliminary flight testing, this design could be used to transport cell culture samples to and from collaborating research labs with a lower probability of cell damage than expected without the use of a protective design.

Throughout this design process, engineers learned to design and build a microcontroller with multiple sensors and amperage requirements. Tracking systems were thoroughly investigated and the engineers learned to track payload systems in real time using aprs tracking methods. The engineers on this project collaborated with engineering and architecture firms to design the protective casing for the payload and learned key elements of the design process including professionalism, CAD design, and fabrication processes. In addition, it was learned that murine myoblast cells are relatively durable and do not require gas exchange for at least 24 hours and can withstand moderate amounts of radiation exposure without significant morphology and vitality changes.

Given unlimited time and resources, this design would benefit from further flight testing, sensors to monitor pH *in vitro* and pressure *in vitro* and in the atmosphere, an accelerometer for more precise flight data, exposing differentiated cells to radiation during flight to more accurately mimic space flight, performing DNA analysis on key protein pathways that experience changes in microgravity, and design implementation on a CubeSat with remote systems monitoring.

Recommendations for Future Work

pH Control

The microcontroller may be used to monitor and control the pH of the media in the culture chambers with a sensor and gas spargers. For *in vitro* cell culture, CO_2 is held steady at 5% in the incubator, which enables the media to buffer the pH.

Air Sparging

Sparging gases such as CO_2 within the flasks could extend the time and altitude of the payload while in flight and enable the media to buffer the pH levels.

Video

Including a camera to take either video or photos of the cells during the flight could be beneficial in the event of a mechanical failure or crash landing. It could also be beneficial to have a camera on the exterior of the payload that could livestream video to a computer. This would be another means of tracking and easy recovery.

Radiation Exposure

In order to better simulate space, exposing the cells to radiation during the flight could generate valuable data on the viability and morphology of the muscle cells during analysis after the flight.

Additional Flight Trials

One launch can be quite expensive, but if more resources available, executing more than one flight trial would help in determining what adjustments are required for maximum height and flight time.

Longer Flight

A longer flight can be facilitated by obtaining a higher gram weight balloon. It will hold more helium gas and would not burst as early in flight as a lower gram weight balloon.

References

Damm, T. B., Richard, S., Tanner, S., Wyss, F., Egli, M., & Franco-Obregón, A. (2013). Calcium-dependent deceleration of the cell cycle in muscle cells by simulated microgravity. *The FASEB Journal*, *27*(5), 2045–2054. https://doi.org/10.1096/fj.12-218693

Friedberg, W., & Copeland, K. (2011, May). Ionizing Radiation in Earth's Atmosphere and in Space Near Earth. *Federal Aviation Administration Report*.

Gillies, A. R., Smith, L. R., Lieber, R. L., & Varghese, S. (2010). Method for Decellularizing Skeletal Muscle Without Detergents or Proteolytic Enzymes. *Tissue Engineering Part C: Methods*, *17*(4), 383–389. https://doi.org/10.1089/ten.tec.2010.0438

He, W., Ma, Z., Yong, T., Teo, W. E., & Ramakrishna, S. (2005). Fabrication of collagen-coated biodegradable polymer nanofiber mesh and its potential for endothelial cells growth. *Biomaterials*, *26*(36), 7606–7615. https://doi.org/10.1016/j.biomaterials.2005.05.049

Jaffe, E. A., Nachman, R. L., Becker, C. G., & Minick, C. R. (1973). Culture of Human Endothelial Cells Derived from Umbilical Veins. IDENTIFICATION BY MORPHOLOGIC AND IMMUNOLOGIC CRITERIA. *Journal of Clinical Investigation*, *52*(11), 2745–2756.

Kulesh, D. A., Anderson, L. H., Wilson, B., Otis, E. J., Mehm, W. J., Elgin, D. M., ... Kearney, G. P. (1994). Space shuttle flight (STS-45) of L8 myoblast cells results in the isolation of a nonfusing cell line variant. *Journal of Cellular Biochemistry*, *55*(4), 530–544. https://doi.org/10.1002/jcb.240550412

Mendoza-Novelo, B., Avila, E. E., Cauich-Rodríguez, J. V., Jorge-Herrero, E., Rojo, F. J., Guinea, G. V., & Mata-Mata, J. L. (2011). Decellularization of pericardial tissue and its impact on tensile viscoelasticity and glycosaminoglycan content. *Acta Biomaterialia*, *7*(3), 1241–1248. https://doi.org/10.1016/j.actbio.2010.11.017

Powers, S. K., Kavazis, A. N., & DeRuisseau, K. C. (2005). Mechanisms of disuse muscle atrophy: role of oxidative stress. *American Journal of Physiology - Regulatory, Integrative and Comparative Physiology*, *288*(2), R337–R344. https://doi.org/10.1152/ajpregu.00469.2004

Simone, N. L., Soule, B. P., Ly, D., Saleh, A. D., Savage, J. E., Degraff, W., ... Mitchell, J. B. (2009). Ionizing radiation-induced oxidative stress alters miRNA expression. *PloS One*, *4*(7), e6377. https://doi.org/10.1371/journal.pone.0006377

Strom, S. C., & Michalopoulos, G. (1982). [29] Collagen as a substrate for cell growth and differentiation. In B.-M. in Enzymology (Ed.) (Vol. 82, pp. 544–555). Academic Press. Retrieved from http://www.sciencedirect.com/science/article/pii/0076687982820867

The Free Beginner's Guide. (n.d.). Retrieved October 10, 2016, from https://3dprintingindustry.com/3d-printing-basics-free-beginners-guide/

Unger, R. E., Huang, Q., Peters, K., Protzer, D., Paul, D., & Kirkpatrick, C. J. (2005). Growth of human cells on polyethersulfone (PES) hollow fiber membranes. *Biomaterials*, *26*(14), 1877–1884. https://doi.org/10.1016/j.biomaterials.2004.05.032

Yatagai, F., Honma, M., Takahashi, A., Omori, K., Suzuki, H., Shimazu, T., ... Ishioka, N. (2010). Frozen human cells can record radiation damage accumulated during space flight: mutation induction and radioadaptation. *Radiation and Environmental Biophysics*, *50*(1), 125–134. https://doi.org/10.1007/s00411-010-0348-3

Flight Prediction. (n.d.). Retrieved December 04, 2016, from http://predict.habhub.org/

Appendix I: Additional Research

Pod Material

Originally, the design included a 3D printed outer capsule to protect the cells. However, this was ultimately not used because of weight restrictions. The following is research about pod materials that was not used in the final design.

There are many popular materials now in use for 3D printing that include plastics, metals, ceramics, paper, biomaterials, and food ("The Free Beginner's Guide," 2014). Plastic materials are most common four forms: Nylon, ABS, PLA, and Laywood. For metals, the most common material is stainless steel powder, followed by aluminum and cobalt derivatives, and titanium powder which is incredibly strong. Gold and silver can also be added to make stronger alloys. Ceramics, paper, biomaterials and food are all still in the early stages of development and are not as common, but can still be used. For this project, plastics were investigated as they are relatively inexpensive and easily attainable. Details of this investigation are discussed in Tables 2, 3, and 4.

Plastics:

Nylon, or polyamide, is strong, flexible, and durable. It is available in powder or filament form and can also be combined with aluminum powder to make alumide and increase strength. It can come in a variety of colors, but is naturally white. It is ideal for snap-fit and friction fit designs and good for high endurance, i.e., casing snaps. Nylon comes in many different subtypes that include: 6/6, 6/12, 4/6, 6, or 12, indicating how many carbons are in one monomer.

ABS, or acrylonitrile butadiene styrene, is a very common plastic that is also known as the lego plastic. It has excellent impact resistance, is easy to machine, paint, and glue, and has good strength and stiffness. It is also relatively inexpensive to acquire.

PLA, or polylactic acid, is very similar to ABS, but it is biodegradable and comes as a resin or filament. It can be colored or be transparent which gives it more applications than ABS; however, it is not as durable or flexible as ABS.

Laywood is a combination of wood and polymer composites. It contains 40% recycled wood particles, which gives it many properties of wood so it can be ground, sanded, or painted. Its thermal properties are similar to PLA, but can be quite expensive.

Table I.1. Physical properties of 3D printing materials.

	Nylon	**ABS**	**PLA**
Chemical Formula	6/6 – $(NH(CH_2)_6NHCO(CH_2)_4CO)_n$ 12 – $(NH_2(CH_2)_{12}O_2)_n$	$(C_8H_8C_4H_6C_3H_3N)_n$	$(C_3H_4O_2)_n$
Molecular Weight	6/6 – 226.32 g/mol 12 – 197.32 g/mol	211 g/mol	72 g/mol
Tensile Strength	90-185 N/mm^2	44 MPa	50 MPa
Thermal Conductivity	0.25 W/mK	0.17 W/mK	0.13 W/mK
Density	1130-1350 kg/m^3	1040 kg/m^3	1250 kg/m^3
Specific Heat	1670-1700 J/kgK	1423 J/kgK	1800 J/kgK
Low Working Temperature	(-40°C)-(-30°C)	-20°C	--
Melting Point	190 °C -350°C	105°C	160°C

Table I.2. Chemical structures of 3D printing plastics.

Nylon 6/6	Nylon 12	ABS	PLA
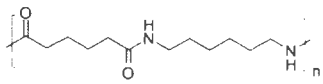	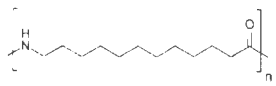	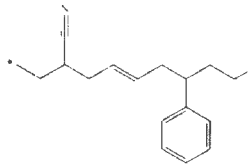	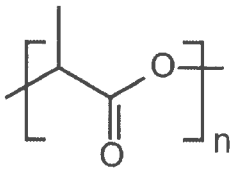

While the material of the pod will be able to insulate the cells within to an extent, the project will also investigate possible insulators. There are many insulators currently available, but they vary in attainability and cost. An insulator that could be wrapped around pod is also being considered because it could protect the pod, scaffold, and cells from damage as the satellite returns to the ground. Table 3 lists several options for insulators.

Table I.3. Insulators and their thermal conductivity and R-values. (Note: the higher the R-value, the better the material is at retaining heat.

Type	Cost	Thermal Conductivity (W/mK)	R-value/in	Notes
Aerogel	$$$	--	--	Many kinds, expensive
Fiberglass	$	0.04	3.1	Cheap, requires PPE
Mineral Wool	$$	0.04	3.1	Effective, not fire resistant
Cellulose	$$	0.23	3.7	Fire resistant, hard to apply
Polyurethane Foam	$$$	0.02	6.3	Light, low density, fire resistant
Polystyrene	$	0.033	4	Waterproof, aka Styrofoam, smooth surface

Type	Cost	Thermal Conductivity (W/mK)	R-value/in	Notes
Natural Fibers	$	--	--	Hemp, sheep's wool, cotton, straw
Cork	$$	0.04	3.33	Easy to find, but not as good a polystyrene
Air Space	--	0.024	~1	Must be completely sealed
Sawdust	$	0.08	2.44	Cheap, easy to find, bad when wet
Silicone	$	0.14	2.35	Cheap, can buy in sheets, protective
Silicone Foam	$$	0.035	2.5-2.6	A little pricier than regular silicone, but a better insulator, protective
Butyl Rubber	$	0.09	--	Slightly harder to find, protective
Natural Rubber	$	0.14	2.20	Readily available, protective

Substrate Material

Polysulfone (PSU) and Polyethersulfone (PES)

Polysulfone has been used in cell culture because it is relatively easy to obtain and has a high surface area. PES and PSU are available in many different forms such as in film, granule, rod, or sheet form. It is easy to machine and can be molded into hollow fibers, which increases the surface area for cell growth as it can also be very porous. It is also popular as a substrate because of its chemical resistance, hydrophobicity, and antifouling properties. Very rarely does the surface need to be treated in order for cell attachment to occur. It is wear resistant because of its strength, flexibility and porosity, indicating it can withstand a crash landing after a balloon flight. It has the option of 76% transparency, but is normally white which is disadvantageous as it is difficult to image cells when the material is in hollow fiber form and not transparent. However, it can also be quite expensive to purchase.

Many different types of cells have been known to grow on PSU and PES, such as glial cells, epithelial cells, endothelial cells, fibroblasts, and osteoblasts (Unger, 2005). Figure 8 shows the growth of osteoblasts on PES. A lot of growth was observed because of the high surface area.

Unfortunately, there may be some problems with growth on hollow fiber membranes. Although growth is generally successful, there are some concerns about the removal of the cells for the Genechip analysis. It is also difficult to image the results of cell growth because the fibers must be cut with a razor.

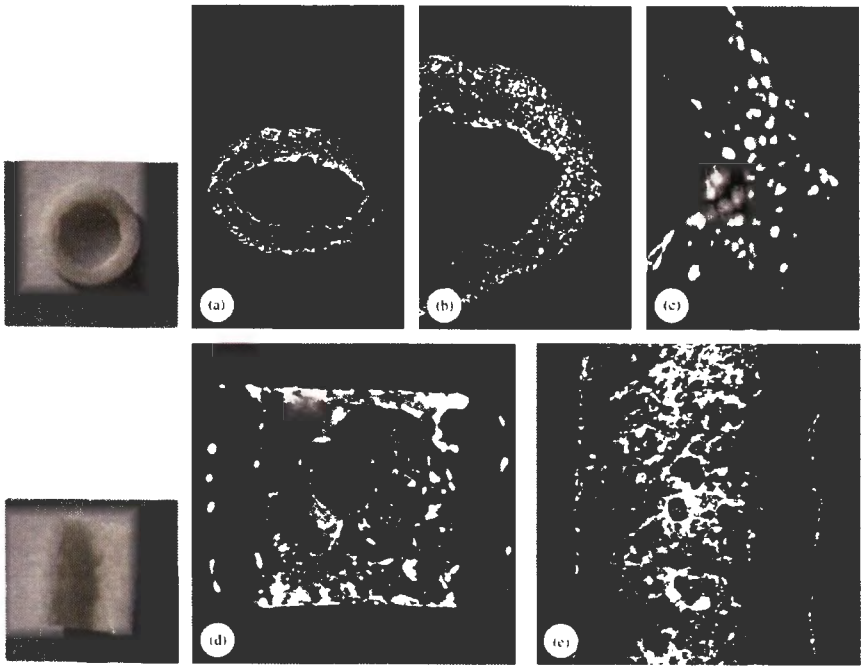

Figure I.1. Growth of cells on the various surfaces of PES. The top images (a–c, 5×, 10× and 20×, respectively) show growth of Calcein-AM stained osteoblast cells (MG63) on the cut surface of diagonally cut PES tubes (image of PES cut across the fiber) and the bottom images of HaCaT cell growth on diagonally cut PES inner (d) and outer surfaces (e, both 10×). Image courtesy of Unger et al[29].

Collagen

He, Wei et al. researched ways to incorporate collagen protein in a nanofiber mesh (NFM) to facilitate endothelial cell growth by pretreating the NFM with oxygen plasma (He ,2005). The NFM was fabricated by electrospinning poly(L-lactic acid)- co-poly(ε-caprolactone) P(LLA-CL 70:30) at 10 kV from a 0.21 mm syringe needle onto coverslips resting on aluminum (He, Ma, Yong, Teo, & Ramakrishna, 2005). The surface of the P(LLA-CL) was modified with air plasma treatment carried out in an inductive coupled radio frequency discharge plasma cleaner for 5 minutes at 30 W to increase the surface hydrophilicity of the material.The treated NFM was immersed in a 0.01 M HCl collagen solution with a concentration of 290 μg/ml at 4°C overnight then dried at room temperature under laminar flow (Figure 9). The amount of collagen coated onto the NFM was measured using the BCA Protein Assay Kit (Pierce, USA) by immersing the

coated NFM in a solution of 0.1 ml PBS and 2 m1 reaction reagent at room temperature for 2 hours. Absorbance was measured at 562 nm then the collagen concentration was calculated from the collagen standard curve.

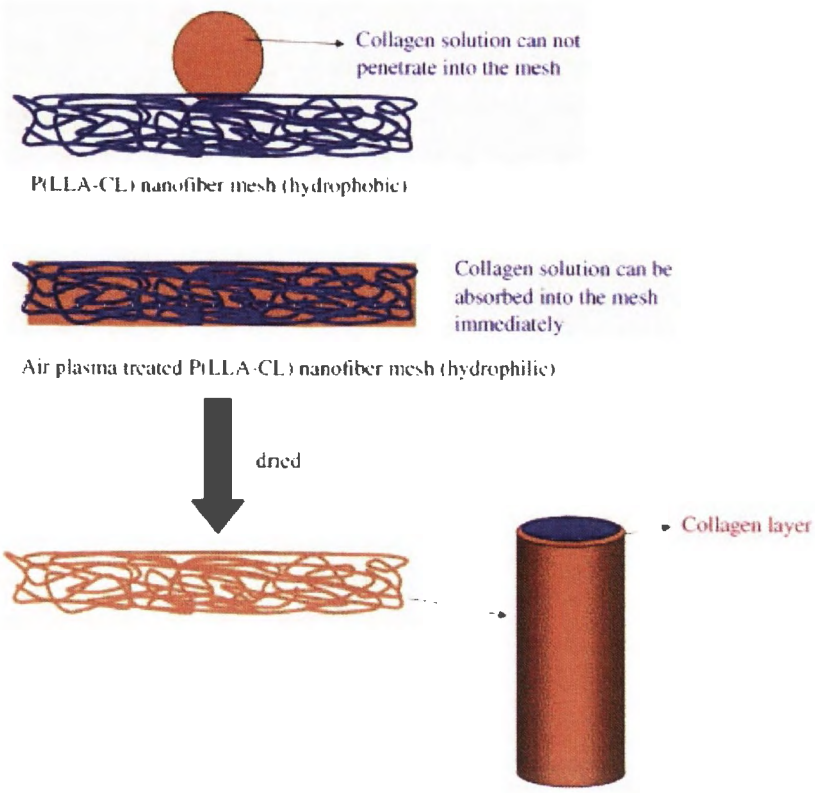

Figure I.2. Schematic representation of the plasma treatment and collagen coating of the electrospun P(LLA-CL) NFM.

Human coronary artery endothelial cells were seeded on collagen-treated NFM at $5x10^4$ cells/cm^2 and treated with EBM 5% FBS medium with 100 units/ml penicillin and 100 µg/ml streptomycin at 37°C, 5% CO_2. Cell morphology was studied by staining live cells with green fluorescent probe 5-chloromethylfluorescein diacetate (CMFDA) and observing under laser scanning confocal microscopy (LSCM). Cells cultured on untreated NFM were rounded instead of a spreading morphology whereas cells cultured on collagen treated NFM adopted a spreading polygonal shape typical of normal morphology on TCPS as seen in Figure 10. Cell viability on collagen treated NFM was higher than untreated NFM but lower than TCPS values after the first 3 days of culture. This research group concluded that air plasma treatment was effective in increasing collagen coating onto nanofiber's surface evenly and the collagen-enhanced endothelialization.

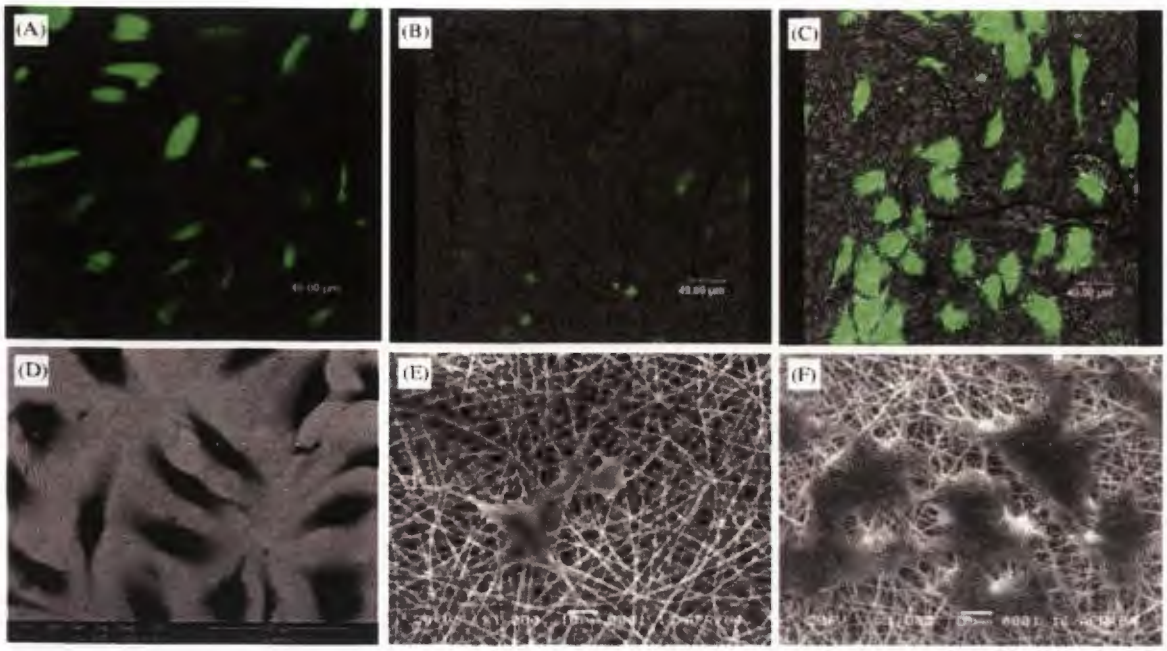

Figure I.3: LSCM and SEM images of endothelial cells cultured on (a, d) tissue culture polystyrene, (b, e) P(LLA-CL) NFM and (c, f) collagen-coated P(LLA-CL) NFM. HCAECs were seeded at a density of 3×10^4 cells/cm^2 and stained with CMFDA for fluorescent observation or fixed for SEM study 3 days later. (He, Wei et al.)

Stephen Strom's chapter in "Methods in Enzymology" details collagen fiber extraction from rat tail vertebrae. These fibers were left to dry at room temperature for 3 hours then sterilized under UV light for 48 hours (Strom, 1982). The fibers were then transferred to 0.1% v/v acetic acid in distilled water and stirred for 48 hours on low speed with a stir bar. The collagen suspension was then filtered through a sterile triple gauze filter to remove any remaining undissolved fibers; undissolved fibers were not found to have adverse effects on cell growth but do allow for easier pipetting. Strom's collagen suspension was used to coat plastic tissue culture plates and prepare collagen gels.

Tissue culture plates were prepared using 2 ml (for a 60 mm plate) of 1:10 dilution of collagen suspension (above) and shaken by hand to ensure a uniform solution distribution. Plates were placed in a dry incubator at 37°C until the plates were dry; approximately 1 - 2 days. Treated plates were stably stored in a humidified incubator indefinitely and used for tissue culture as seen in Figure 11.

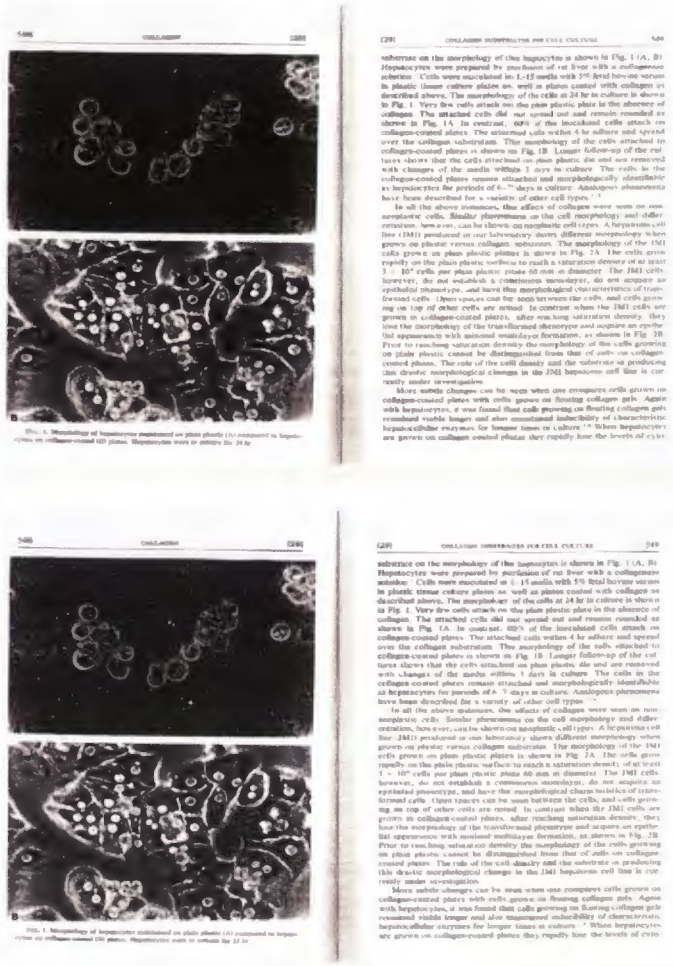

Figure I.4. Morphology of hepatocytes maintained on plain plastic (A) compared to hepatocytes on collagen-coated plates (B) over 24 hours. (Strom).

Collagen gels were prepared by simultaneously raising the ionic strength and pH of the solution so that the protein fibers precipitate *in situ*. Waymouth MB 752/1 10X was supplemented with 20 g/L FBS and mixed with 0.34 M sodium hydroxide and collagen solution on ice at volume relations of 2.66:1.10:17 Waymouth, sodium hydroxide, and collagen respectively. 2 ml of this solution was added to a 60 mm diameter plate and left at room temperature until a gel was formed; approximately 5 - 10 minutes. Gels were stable in a humidified incubator for at least 1 month. Cells were added to gels in culture plates to cover approximately 60% of the gel surface.

Polystyrene (PS)

Many cell culturing flasks are made of polystyrene, making it an excellent control substrate. Some of its many applications include tissue culture trays, test tubes, and petri dishes. It is advantageous because it is easy to sterilize and relatively inexpensive. It is also 100% transparent, making it easy to image cells. However, its disadvantages include its

extreme flammability and inability to be molded into hollow fibers. Table 5 shows a comparison of these properties.

Table I.4: Comparison of substrate properties. Values retrieved from http://www.goodfellowusa.com/

	Polyethersulfone	**Polysulfone**	**Collagen**	**Polystyrene**
Thermal Conductivity (W/mK)	0.16	0.26	0.34	0.13
Upper Working Temperature (C)	180-220	150-180	65-70	50-95
Lower Working Temperature (C)	-110	--	28	--
Radiation Resistance	good-fair	good	minimal	good
UV Resistance	fair	poor	fair	poor
Water Absorption (24hr) (%)	2.2 (0.4-1)	0.4		0.06
Density (g/cm^3)	1.37	1.24	1.17	1.05
Specific Heat (kJ/kgK)	1.1	0.53	0.96	1.2
Tensile Strength (MPa)	70-95	70	--	52
Tensile Modulus (GPa)	2.5	2.48	--	3.1
Hardness	M88	M91	--	M75
Cost	$$$		$$	$

Appendix II: Materials and Methods

Decellularization of Muscle Tissue

The most common methods of tissue decellularization are detergent and enzymatic based treatments that result in extracellular matrix (ECM) degradation, leaving the collagen structure unsuitable for biochemical analysis of new tissue growth (Mendoza-Novelo, 2011) (Cebotari, 2010). An unused method that utilizes osmotic shock and actin and myosin depolymerization does not require any proteases or detergents is detailed in the appendix (Gillies, 2010).

Materials

- 50 nM latrunculin B
- high-glucose DMEM
- 0.6 M potassium chloride
- 1.0 M potassium iodide
- DNase I

Methods

*All steps are performed at room temperature with agitation unless otherwise specified.

1. Incubate muscle tissue in 50 nM latrunculin B in high-glucose DMEM for 2 hours at 37°C
2. Wash tissue with distilled water for 15 minutes
3. Incubate tissue in 0.6 M potassium chloride for 2 hours
4. Wash tissue with distilled water for 15 minutes
5. Incubate tissue in 1.0 M potassium iodide for 2 hours
6. Wash tissue in distilled water overnight
7. Repeat steps 2 - 6
8. Incubate tissue in DNase I for 2 hours
9. Wash tissue in distilled water for 2 days, change water daily

SEM fixation of biological tissues and imaging

Before a biological sample can be imaged by SEM, it must be fixed with chemicals to remove all the water. This method enables the sample to withstand low pressures of up to 0.08 Torr (10.6 Pa or 105 x 10-6 atm) (Jaffe, 1973). This cell analysis method was unused and is detailed in the appendix section.

Materials

- 2% buffered glutaraldehyde
- 0.1 M Hepes buffer
- 100% Ethanol
- Hexamethyldisilazane

Methods

Fixation:

(Note: Always wear gloves when handling the sample to prevent chamber contamination)

1. Fix sample with 2.5 mL of 2% buffered glutaraldehyde overnight
2. Rinse sample with Hepes buffer 3 times for 5 minutes with gentle agitation
3. Rinse sample with 50% ethanol for 10 minutes with agitation; 2 times
4. Rinse sample with 70% ethanol for 10 minutes with agitation; 2 times
5. Rinse sample with 95% ethanol for 10 minutes with agitation; 2 times
6. Rinse sample with 100% ethanol for 15 minutes with agitation; 2 times
7. Fix sample with (2 parts 100% EtOH : 1 part HMDS) for 15 minutes
8. Fix sample with (1 parts 100% EtOH : 1 part HMDS) for 15 minutes
9. Fix sample with (1 parts 100% EtOH : 2 part HMDS) for 15 minutes
10. Fix sample with HMDS for 15 minutes; 3 times
11. Allow HMDS to evaporate overnight in fume hood

Imaging:

1. Cut sample to 10 mm x 10 mm
2. Attach sample to sample holder using double-sided copper tape
3. Vent SEM
4. Insert sample into sample holder
5. Close SEM drawer and pump vacuum to 0.96 Torr (Low vacuum)
6. Move sample to beam area, raise within 10 mm of beam exit
7. Settings should be: 10 kV beam, spot size = 4, bias = 64.5
8. Turn beam on
9. Increase magnification to 500X, focus on an object then link sample distance
10. To render an image for publications, cha nge resolution to 1024 x 768, dwell time to 15 seconds, and line integration to 2; pause image collection

Appendix III: Decisions Not Used in Final Product

Radiation Shielding

To control for the effects of upper atmosphere radiation on cell changes, one flask was shielding inside the payload. The interior insulation, aluminized mylar, shields the cells from both alpha and beta particles so that the only radiation effects come from gamma rays. The decision process for the material used for shielding cells from gamma radiation is detailed in Table 12.

Table III.1. Decision matrix for gamma radiation shielding.

Material	Weight	Shielding Ability	Notes
Solid lead	High	High	It takes approx. 1 inch of lead on all sides to completely shield a material
Lead foil	Medium	Medium	A flexible lead sheet - similar to aluminum foil
Water jacket	High	Medium	It takes approx. 2 inches of water on all sides to completely shield a material

It was decided to use lead foil to shield the control cell flask from gamma radiation because it is relatively lightweight and will provide enough shielding to make a noticeable difference between the control and exposed flasks.

Author Biography

Annelise Dykes recently completed the requirements for USU's Bachelor of Science in Biological Engineering. As a student at USU, she served as Vice President of the Society of Women Engineers and participated in Engineers without Borders. She organized [something you did in SWE, I guess]. She also researched how the genetics of the immune system affect Autism with Dr. Anthony Torres and how Raman spectroscopy could be used to identify Mycobacteria with Dr. Elizabeth Vargis. Annelise plans to use her experience to work in data analytics.

Personal Reflection

This project turned out to be much more difficult than our group originally anticipated. The most difficult thing about the design process was that things went wrong in completely unexpected ways. Every time that happened, the problem had to be fixed, and sometimes the problems had to be fixed quickly because we were close to a deadline.

Possibly the most important thing I learned from this project was the importance of communication. At times the instructions and expectations for the project were not clear, which made it difficult to complete the work as expected. I would have appreciated the opportunity to communicate more regularly with our instructor so that we could have been able to plan our project more easily.

I also learned a lot about writing in this project, which was unexpected. During the second semester of the senior design course, the Biological Engineering department hired Jolynne Berrett to assist with the report writing. I never expected her to be so helpful. Our group relied on our weekly meetings with Jolynne to make sure the report was being written well. In those meetings, we learned a lot about the structure of writing, how to lead into the next sections, making the whole report cohesive while still writing sections that could stand alone, and how to effectively communicate our point to our audience. I never considered myself a particularly bad writer before this experience, but I learned that I had so much room for improvement. The weekly meetings with Jolynne allowed everyone in our group to become better and more efficient writers.

This project also gave me hands-on experience in a few things that I had never done before. One of my roles on my senior design team was to design and program a microcontroller. Before I worked on this, my experience with circuit design was very limited. I had only made simple circuits in electronics labs, and they always worked exactly as predicted. The circuit I designed for the microcontroller was different because I had to work for a very long time to get all the parts to work correctly. After I got the circuit to work, I was able to write a program for the microcontroller that made it read information from the sensors and record data. This was one of the most rewarding parts of working on this project, because it was the first time I had used the knowledge from my general engineering classes to do something on my own.

The final flight of the balloon was also very exciting. We were lucky to have some amazing people to help us, including Dr. Kevin Reeve and Stanley Wellard. Dr. Reeve had tracked balloon launches before, and helped us recover our payload safely. Stanley Wellard had launched many weather balloons to collect data for the Space Dynamics Laboratory, so he made sure we had everything we needed to get the balloon safely into the air and helped us with the launch. The number of things that had to come together to make this project work was amazing. There were a lot of parts of the launch and recovery that could have gone wrong, and if that had happened, the project would have been unsuccessful.

At the end of the capstone project, I was impressed with the work we were able to do. During the year when we had worked on our project, I was busy being stressed and trying to figure out how to make all the different pieces fit together. When we started this project, none of us had ever designed anything from start to finish. It was nice to realize that we could apply what we had learned over the last four years, and combine different bits of knowledge into our final design.